DYNAMIC ANALYSIS OF FLEXIBLE MECHANISMS WITH CLEARANCE

by

Mona Abdullah Hassan Ahmedalbashir

A Thesis Presented to the Faculty of the
American University of Sharjah
College of Engineering
in Partial Fulfillment
of the Requirements
for the Degree of

Master of Science in
Mechanical Engineering

Sharjah, United Arab Emirates

November 2016

Approval Signatures

We, the undersigned, approve the Master's Thesis of Mona Abdullah Hassan Ahmedalbashir

Thesis Title: Dynamic Analysis of Flexible Mechanisms with Clearance

Signature	**Date of Signature** (dd/mm/yyyy)
_____	_____
Dr. Lotfi Romdhane Professor, Department of Mechanical Engineering Thesis Advisor	
_____	_____
Dr. Jin Hyuk Lee Assistant Professor, Department of Mechanical Engineering Thesis Committee Member	
_____	_____
Dr. Rami Hawileh Professor, Department of Civil Engineering Thesis Committee Member	
_____	_____
Dr. Mamoun Abdel Hafez Head, Department of Mechanical Engineering	
_____	_____
Dr. Mohamed Guma El-Tarhuni Associate Dean, College of Engineering	
_____	_____
Dr. Richard Schoephoerster Dean, College of Engineering	
_____	_____
Dr. Khaled Assaleh Interim Vice Provost for Research and Graduate Studies	

Acknowledgments

First, I would like to express all my gratitude and thanks to Dr. Lotfi Romdhane, my advisor, for his guidance, continuous support and encouragement throughout the thesis progress. I am also, very grateful for sharing his treasured knowledge and precious suggestions. Also, I would like to thank my committee examiners; Dr. Jin Lee and Dr. Rami Hawileh for their advice and help.

I would like to extend my appreciation to all MCE faculty members for giving me the opportunity to do my Master's program and work as a graduate teaching assistant in such a great university, the American university of Sharjah. I would also like, to thank all CEN faculty and staff members, especially Ms. Salwa Mohamed for her assistance and guidance.

My deepest gratitude and appreciation go to my dear husband, Eng. Samir Nour, for his patience, kindness, understanding and support over the past two years. Without his encouragement, this work would not be completed. Furthermore, I would like to express my sincere thanks to my parents; Dr. Abdullah Albashir and Dr. Nourelhuda Elshafi, and my family for their thoughtful prayers and care.

In addition, I would like to thank Mr. Kent Bernales Roferos, the Mechatronics lab instructor for his immense assistance during the experimental phase of the thesis. Finally, I want to thank all my friends and colleagues at AUS, and my especial thanks goes to Amr Omar, Wahib Salim and Afsoun Koushesh for their support and for all the good times we spent together.

Dedication

I dedicate this thesis to the memory of my mother's aunt "Haboba Zainab" for helping my parents in raising me and my siblings up and being so kind and thoughtful; may she rest in peace and may Allah bless her soul with His mercy.

To my beloved parents and family for their unconditional love and continuous support.

To my beloved husband for his love and inspiration.

Abstract

This research is focused on studying the dynamic behavior of a four-bar mechanism with clearance. The presence of clearance in a revolute joint induces impacts between the journal and the sleeve. Therefore, it causes vibration, noise and decreases the efficiency of the mechanism. Two different methods are proposed to eliminate the undesirable effects of clearance in the joint through simulations and experiments. The first method, that is used to eliminate these impacts, relies on attaching a spring to a rigid four-bar mechanism. The impacts are predicted by monitoring the moment of the reaction force in the joint with clearance using MATLAB software simulations. It is shown that the impacts could be easily eliminated using adequate and optimized spring parameters. The optimization of the spring parameters is performed to keep the positive effects of adding the spring (eliminating the impacts) and to minimize its negative effects (high maximum input torque and its high fluctuations). The second method aims at studying the dynamic behavior of the mechanism with a flexible coupler link. The dynamic analysis of the flexible mechanism is investigated using two different materials of the coupler link (aluminum and steel) with two different thickness values for each material (3 and 4 mm for aluminum and 1.5 and 2 mm for the steel). The rigid mechanism is considered in this case with a coupler link made of steel with 5 mm thickness to highlight the difference between flexible and rigid mechanisms. The deformation of the flexible coupler links (using ideal joints) is investigated by measuring the strain values at three different speeds (277, 415 and 554 rpm). The obtained results show that the strain values are significantly affected by the crank speed and the thickness of the links. Experimental tests are performed to measure the accelerations for the follower of the four-bar mechanism using rigid and flexible coupler links. These measurements are done for the case of ideal joint (no clearance) and realistic joint with a clearance of 0.5 mm and 1 mm sizes at the three mentioned speeds for each case. The experimental results are validated through simulation tests using ADAMS software. These results confirm that the flexibility of the coupler has thus a role of a suspension for the mechanism.

Search Terms: Joint with clearance, Four-bar mechanism, Flexible coupler, Spring, ADAMS, Free motion.

Table of Contents

List of Figures

List of Abbreviations

ADAMS	Automated Dynamic Analysis of Mechanical Systems
ANCF	Absolute nodal coordinated formulation
DSS	Deployable space structure
GA	Genetic algorithm
GRNN	Generalized regression neural network
LHS	Latin hypercube sampling
MLSD	Massless-link/spring-damper
PSO	Particle swarm optimization
RBF	Radial basis function
TBS	Tripod-ball sliding joint
VEMA	Virtual experimental model analysis

Chapter 1: Introduction

This thesis aims to study the dynamic behavior of a four-bar mechanism with clearance in the joints and flexible links. Several works in the literature addressed this problem. Some of these works were limited to only simulation tests while others were only considering rigid cases. In this research, the experimental study investigates the effect of several parameters on the dynamic behavior of the mechanism; the size of the clearance, the type of the material, the speed, and the geometry are some of these parameters. The parameters to be measured are the acceleration of some points on the mechanism, the strain in the flexible link, the speed and the current of the driving motor. Through these measurements, the dynamic behavior will be evaluated and compared to the simulation results.

1.1 Overview

High speed machines are fairly common in the industry. The dynamic behavior of high speed machines can be critical, especially when they are subjected to high loads. The case of high speed presses is an example of machines with both high speeds and loads. The quality of the parts, which are made by these presses, is highly affected by the high level of vibration due to clearance in the joints and the deformation of the elements. Four-bar mechanisms are found in a wide range of industrial machines. Studying their dynamics could help in better designing these machines [1].

The dynamic analysis of multibody systems attracted several researchers ([2], [3], [4], [5], [6]). In general, the joints of these mechanisms are considered as ideal. However, as a result of manufacturing processes, material deformation and assembly errors, the presence of joint clearance becomes inevitable. The effect of joint clearance can be neglected if the size of these clearances is quite small. However, as the mechanism processes, the size of clearances can increase. This clearance affects the mechanism by causing vibrations, noise and a decline of the mechanism efficiency. The severity of these vibrations depends on the size of the clearance and the type of the joints. Moreover, clearance may cause low motion precision and degradation of the mechanism life-span [7].

As a consequence of clearance in the joint between the journal and the bearing, three types of motion are observed, i.e., contact mode, where the journal and the bearing are in contact; free flight mode, in which the journal moves freely inside the bearing;

and impact mode, which occurs in the termination of the flight mode. When the clearance appears in systems having only rigid bodies, the impact forces in the joints with clearance may have high magnitudes, which cause a high level of vibration and noise [8]. Adding a certain flexibility of the links can have damping effects of these vibrations, which improves the dynamic behavior. However, such flexibility can yield a certain deviation of the links from their nominal locations, which can generate errors in locating the different elements of the systems. These errors can impede the correct functioning of the systems, in some cases [9].

The problem of joint with clearance is an attractive topic that grasped a significant attention due to its serious effects on the mechanisms. The main difficulty comes from the nonlinear and non-continuous model that describes this type of systems. The joint with clearance can be considered as a unilateral contact joint where the reaction force is used to maintain this contact. However, when this force turns zero or negative the contact is lost and the joint is in a free flight mode. Then, high impacts are generated by a collision usually immediately after the free flight phase. Choosing suitable models to consider this loss of contact is an essential step in modeling joint with clearance. Hertz model is one of the most commonly used models to deal with such a problem [10].

Experimental validation of the simulation results is extremely desirable due to the complexity of the theoretical models. As a consequence, the results become more reliable only when they are confirmed experimentally [11]. The dynamic of the system and the measured signals have low magnitudes and high frequencies which make the selection of suitable sensors one of the sensitive issues in building experimental setups. Accelerometers are mostly used to measure the acceleration because of their high sensitivity and high dynamic response. Strain gages can be also used to detect the deformation of the links [12].

1.2 Research Significance

As seen above, the effect of clearance was considered widely in the literature. However, there are some observed limitations upon which the objectives of the current study are based on. These limitations include:

- Experimentation studies are still limited.

- The flexible link method, addressed in the literature ([13], [14], [15]) was implemented using only one coupler stiffness value, which did not give the best desired results.
- Considering the effect of clearance size needs to be emphasized more.

1.3 Thesis Objectives

The objective of the current research is to investigate the effect of joint with clearance on the dynamic behavior of a rigid and flexible four-bar mechanisms using simulations and experimental validation. Several parameters are studied, i.e., material type, thickness of the coupler, clearance size and the crank speed. Two materials are used, steel and aluminum. The mechanism is modeled using ADAMS and the model is validated through experimentation. The main objective of this study is to assess the effect of the flexibility of the coupler on the dynamic behavior of the mechanism with clearance.

1.4 Thesis Organization

Chapter 1 introduces a general idea about the effect of joints with clearance on the dynamic behavior of the mechanism. An overview of the literature related to the different methods used to overcome the problem of clearance in the joint is provided in Chapter 2. Chapter 3 discusses the description and the dynamic modeling of the four-bar mechanism, the modeling of the clearance and the improvement of the dynamic behavior of the four-bar mechanism after attaching a spring through simulation and experimental tests. Chapter 4 investigates the dynamic analysis of a flexible four bar-mechanism with ideal joints using different stiffness values. Chapter 5 presents the simulation and the experimental results of the flexible mechanism with realistic joints (Joints with clearance) and indicates how the flexibility of the coupler effects the overall behavior of the mechanism. Then, the research is summarized and the recommendations and future contributions are provided in Chapter 6.

Chapter 2: Literature Review

In order to provide a basis for studying the dynamic behavior of a mechanism with joints with clearance, a number of related papers have been briefly summarized in this chapter.

2.1 Flexible Coupler Link with Joint Clearance

The flexible link technique proposed in [13] investigates the effect of joint clearance on the dynamics of a rigid and flexible slider-crank mechanism. The authors studied the mechanism's responses in both cases using simulation and experiments. The model was built using ADAMS software. Modeling of the contact has been done using the impact function, which calculates the contact force using ADAMS function library. The simulation results were validated by setting up an experimental test. The obtained results show that in the presence of clearance the flexibility of the coupler link improved the performance of the mechanism significantly.

The work in [8] also focuses on studying and analyzing nonlinear dynamics of a slider-crank mechanism with a flexible coupler having cracks and a slider with clearance. The flexible link and the crack were modeled using successive equal rigid rods connected with massless rotational springs. The clearance of the mechanism was simulated using impacts. The stability of the system was investigated using Lyapunov exponents, which provides a measure of the sensitivity of the system to its initial conditions.

The interconnected rigid and flexible components were examined using different angular velocities. Results show the different types of motion between the guide and the slider, which are: continuous contact, free flight, impact and direction change between slider and guide. There are many peaks that were observed at various time positions as a consequence of the clearance of the slider and the higher acceleration peaks caused by the inertial forces. The analysis of the type of dynamic evolution of the slider-crank mechanism showed that the system has changed from regular behavior to chaotic behavior.

The idea of elastic linkage was used in [14] to analyze the non-linear behavior of a rigid link with clearance through the phase portraits and Poincare maps. The analysis included improving a unified dynamic model between the separation and collision processes for the flexible linkage mechanism by choosing two sets of generalized

coordinates. This model incorporates the effects of rigidity and elasticity coupling where the angular velocity was considered as variable in the operation. The dynamic equations of motion were derived using Newton's second law and the deflection equation of the coupler link was derived using Finite Element method.

The dynamic analysis of the flexible four-bar mechanism with radial clearance was studied and the numerical results were discussed in [14]. The results show that the mechanism performance without radial clearance is much better than a mechanism with excessive radial clearance. The mechanism with flexible links has much less number of peaks of impact forces than the mechanism with only rigid links.

The same method was also proposed in [15]. The main objective in this work was to analyze the dynamic behavior of a mechanism with clearance for a high-speed press using a flexible slider-crank mechanism. The model of the slider-crank mechanism with clearance for a high-speed press system was built using ADAMS software. The dynamic analysis was based on a nonlinear spring-damping model taken from Hertz contact theory and the modified coulomb friction model. Two of the revolute joints were considered as ideal and the other two took into account the clearance between the crank shaft and the coupler and between the coupler and the slider. Modeling of the friction force was done using LuGre friction law as the stick-slip friction may exist in the revolute joint. The simulation was done for different sizes of the clearance. The results show that the dynamic responses of the mechanism were affected significantly when the size and the numbers of clearance increase in the rigid case while in the case of a flexible link all responses were highly deaden.

2.2 Balancing and Link Flexibility

The main emphasis of the work presented in [16] was to experimentally investigate the joint clearance effects on a planar mechanism, and to minimize these effects using link flexibility and balancing methods. The adjacent mechanism links were assumed to be connected to each other by revolute joints. The original Hertzian model was modified to include the energy dissipation due to internal damping. To analyze the system, an experimental test rig was set up where Aluminum links were used. In order to check how the balancing and link flexibility characteristics can decrease the undesired effects of joint clearance, three accelerometers were used to measure the vibration of the main frame for the cases of balanced and unbalanced, and rigid and flexible mechanism configurations.

From the obtained results, it was observed that the accelerations were nearly periodic with peaks due to impact forces between the journal and the bearing. The effect of these forces was suppressed by the balancing of the mechanism. Also, the link flexibility played an important role in decreasing the vibration peaks.

2.3 Prediction of Vibration Characteristics of Mechanisms having Joint Clearance using Neural Network Method

The work presented in [17] investigated the effect of joint clearances on the mechanism vibration by setting an experimental test rig. Experimental measurements were performed for different sizes of clearance. Two types of neural networks were implemented to predict and estimate the system vibration, i.e.: Radial basis function (RBF) and Generalized regression neural network (GRNN). The first method uses an input matrix that consists of a series of time, clearance sizes, running speed and material type of the mechanism. The Generalized regression neural network (GRNN) consists of four layers; input layer, pattern layer, summation layer and output layer.

In the experimental study the vibration characteristics of the system were investigated using a planar mechanism model. Three accelerometers were used to measure the vibration of the main frame. Three different sizes of clearances were used for the experimental study. The observed results show that vibration characteristics were mainly periodic and the peaks at the vibration amplitude come from the different types of motion: the impact and free flight. GRNN provided poor convergence ability for all the simulations unlike the RBF neural network, which succeeded in predicting the bearing vibrations at different running speed conditions and system characteristics.

2.4 Effect of Lubrication of the Joints with Clearance

The research in [18] deals with the dynamic behavior of mechanisms using the lubrication at the joint with clearance. Studying the dynamic behavior of lubricated joints requires filling the clearance with lubricant, which results in generating a pressure distribution and hydrodynamic forces. The studied mechanism is a planar slider crank mechanism with a clearance at the piston revolute joint. The equations of motion were derived using the Lagrange method. The contact model used in this problem was proposed by Lankarani and Nikravesh [18], where the contact force consists of a dissipative term proportional to the impact velocity of the bodies. Two models of the hydrodynamic lubrication were studied: the first model introduces a direct solution of

low computational cost and the second model studies the effects of the acceleration of the lubricant fluid imposed on the movement of the mechanism.

The dynamic model of the slider-crank included a simple model of internal combustion engine. The simulation includes two different conditions: without and with an external load on the piston. The simulation results of two different models were compared. The results show that the second lubrication model does not insure the support of the piston–pin system for hydrodynamic lubrication in the simulated interval of time. Therefore, it is important to develop a more realistic model of hydrodynamic lubrication that has the ability of reproducing the behavior of the piston–pin contact.

The lubrication of the joints method proposed also in [19] focuses on studying the dynamic behavior and the analysis of flexible spatial multibody systems with clearance and lubricated spherical joints. The equations of motion were derived using the ANCF (Absolute nodal coordinated formulation). The evaluation of the inertia impact forces was done using the modified Hertzian-based contact law, which is a continuous contact-impact taking into account the energy lost in the form of hysteresis damping. The modified Coulomb's friction law was used to consider the friction in the joints. The model used for the spherical joint with clearance derived the lubrication forces using the corresponding Reynold equations. The dynamic simulation considers two cases: ideal joints, and lubricated joints with clearance. Two spatial multibody systems were analyzed: open-loop system; (the spatial double pendulum), and a closed-loop system (spatial four bar mechanism). The results show that the lubricated joints performed close to the ideal joints as the fluid lubricant prevents the presence of the direct ball-socket impact.

2.5 Optimization Methods

The primary objective of the work presented in [20] was to improve the accuracy of the dynamics response of a mechanism with joint clearance using optimization. The planar joint clearance model was used to model a reciprocating compressor. A two-stage reciprocating compressor with four joints with clearances was modeled using ADAMS software. The dynamic equations of this slider-crank mechanism were established using the Lagrange method. The joint clearance was modeled using Hertz contact force model. This model is the best-known contact force between two spheres of isotropic materials, where the normal contact force was separated into an elastic component and a dissipative one. The friction force uses a continuous friction force-

velocity relationship in order to stabilize the integration of the dynamic equations. The results show that the contact force values peaked and dropped immediately to zero, which corresponds to an impact followed by a free flight motion in the joints. The simulation results were validated using the experimental tests.

Optimization techniques, which were also used in [9] aimed at studying the dynamic behavior of a planer slider-crank mechanism with rigid links in the presence of clearance in the revolute joint between the slider and the connecting rod. The objective of the research was to maintain the contact between the journal and the bearing using a mass distribution of the moving links. The equations of motion for the slider-crank mechanism were derived using the Lagrange method. In the optimal design, the dynamic performance in the presence of clearance was modified using mass re-distribution of the moving links in order to eliminate the impact force by keeping the journal and the bearing in contact. A slider-crank mechanism was used to illustrate the efficiency of the optimization and the problem solved using PSO (Particle swarm optimization) algorithm with constraints.

The dynamic simulations were compared for both optimal and original designs by plotting the slider acceleration, the angular acceleration of the connecting rod, the contact force, and the locus of the journal center relative to the bearing center. The results show that the maximum values of the slider acceleration and the values of the contact force in the joint with clearance, and the input torque were reduced significantly for the optimal design compared to the original design.

The main idea of the study presented in [21] was to illustrate the effect of various objective functions with several design variables on the dynamic response of a mechanism with joint clearance using multi-objective optimization utilizing the Kriging meta-model. The Kriging-meta-model, which is based on the design of experiment method, was used to replace the computationally intensive simulations by a simpler, yet effective model.

The slider-crank mechanism was modeled using ADAMS software and the number of the sampling points, needed for the Kriging model, was determined using the Latin Hypercube sampling (LHS) method. The multi-objective optimization was done using different sets of objective functions and design variables. The revolute joint clearance was modeled as a pin-in-hole with dry contact using the Hertzian contact force model with hysteresis damping.

The dynamic response of the slider-crank mechanism with revolute joint with clearance was studied for the multi-objective optimization, while the meta-model was developed to optimize and analyze the simulated results. These responses for the slider-crank mechanism were validated with the experimental results and the simulated results reported in the literature. The meta-model results show that the objective functions were quite sensitive to the clearance size, and that the multi- objective optimization indicated similar results with the ones obtained from the meta-model.

2.6 Massless-Link/Spring-Damper (MLSD)

In order to predict the clearance behavior, two methods were reported in [22]: The massless-link method and the spring damper method. The massless-link models the clearance by adding a link of zero mass with a fixed length equal to the radial clearance between the pin and the journal. The spring damper method replaces the gap due to the clearance by a spring-damper unit to model bearing surface elasticity. Adding these two methods provides a method called massless-link/spring-damper (MLSD). A four-bar mechanism with a clearance in the joint was studied using the combined MLSD model. In order to determine the contact loss boundaries, the dynamic equations were numerically integrated over a wide range of speeds using ADAMS software.

The results confirmed that the time required for the numerical integration using MLSD model was four time longer than the time needed using massless-link equations and almost one hundred times more than the time required for the zero-clearance equations. The MLSD model predicted the chaotic behavior just before the contact loss. For high stiffness values, the contact loss happened at crank speeds above 253 rpm, whereas, the damping had almost no effect on the chaos happening or the location of chaotic boundaries.

2.7 Finite Element and Virtual Experimental Model Analysis (VEMA)

The work presented in [23] focused on investigating the dynamic behavior of deployable space structure (DSS) with joint clearance using link flexibility and finite element method. Deployable structures are special types of deployable mechanisms, which are capable of supporting loads by transforming from a closed compact to an expanded format with larger size or surface. The finite element method was used to model the joint clearance and the model was built using ANSYS software. A virtual experimental model (VEMA) method was proposed to study the effects of joint clearance and link flexibility, which proved to be time and cost efficient method.

The transient analysis and frequency response of the structure were provided to obtain the displacement response data. The modal parameter identification method was used to obtain, the modal parameters of the structure. Experimental validation was carried out to verify the VEMA method, which was found to be cost and time efficient approach to obtain the dynamic characteristics of the DSS. The analysis results show that, the joint clearance and gravity affect the dynamic characteristics of the DSS.

2.8 Hybrid Nonlinear Continuous Contact Force Model Method

The work in [24] presents a study of the dynamic behavior of dual-axis positioning mechanism of a satellite antenna with joint clearance using a new hybrid nonlinear continuous contact force model. The system was analyzed using ADAMS software. The study of the dual-axis positioning mechanism with clearance in the joints was done using the clearance vector model. This method represents the potential real movement and the relative position between the journal and the bearing. It can also specify whether the journal and the bearing of the joint are in contact or not. The contact journal bearing in the revolute joint was modeled using the new hybrid nonlinear contact force model. The friction response between the journal and the bearing was represented using the modified coulomb friction model.

The simulation was carried out for both the ideal mechanism and the real mechanism with clearance. The plots of the dynamic responses show that the angular velocity curve of the dual-axis positioning mechanism is very smooth in case of no clearance, while it has some deflections from the ideal mechanism and shaky shape in case of presence of clearance. Also, the angular acceleration in case of clearance showed shaky responses and a higher amplitude than the ideal mechanism response. In the research [24], four cases of different clearance sizes were studied to analyze the effect of the clearance size. The results indicate that the deviation of dynamic responses increases with the increase of the clearance size.

2.9 Stabilizing the Mechanism using Feedback Control Method

In the work presented in [25], the delayed feedback control was used to reduce the effects of the joint clearance on the slider-crank mechanism dynamics. The equations of motion for a slider-crank mechanism with clearance were derived using Lagrange method. The motion occurs in two modes: the contact and noncontact mode. A chaotic motion happened as a consequence of impacts which was followed by rebounds between journal and bearing in the joint with clearance. This motion caused

high peaks in the slider acceleration and the crank moment. Poincare map and fractal dimension were used in order to investigate the chaotic motion. By controlling the mechanism using Pyragas method, the unstable periodic motion was stabilized and the loss of contact was eliminated. As a result, the journal and bearing were kept in permanent contact and the mechanism provided smother responses.

2.10 Bifurcation Analysis Method

The main idea presented in [26] was to study the non-linear behavior of a slider crank mechanism with clearance in the revolute joint between the slider and connecting rod. The bifurcation analysis method was used to provide some stability ranges for the clearance size. To demonstrate the system behavior in discrete state space, Poincare portraits were applied, which have a crucial role in understanding nonlinear behaviors of dynamical systems.

The dynamic equations of motion were obtained using Lagrange method and the solutions were found through applying the fourth order adaptive Runge– Kutta method. The continuous contact force model, proposed by Lankarani and Nikravesh [26], was used to calculate the normal contact force between the journal and the bearing. The friction effect was found using the Ambrosio model.

In order to understand the effect of the clearance size on the system behavior, the bifurcation diagrams response was plotted versus the clearance size and the results show that, in case of small clearance sizes the mechanism behavior transforms from chaotic to periodic while in case of large clearance sizes sudden changes from periodic to chaotic happened.

2.11 Tripod-Ball-Sliding Joint

The work presented in [27] included analytical and experimental investigations of the dynamic performance of a crank-slider that has additional motion, reacting forces, driving torque and contact state of the tripod-ball sliding joint -TBS joint- with clearance (Figure 1). The mathematical model of the TBS joint was presented and the equation of motion in full-scale was derived using Kane formulation. The new concept of basal system was introduced, in which there is no force exerted in the TBS joint when it is in the free flight mode and the system has invariable topological structure.

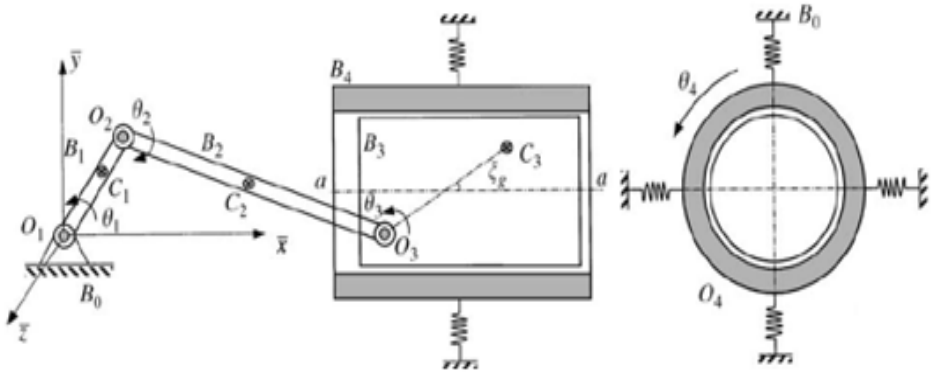

Figure 1: The crank-slider mechanism with clearance in the TBS joint [27]

Experimental tests were carried out to measure the effects of the clearance in the TBS joint. The numerical and experimental results show that the stability of mode-change was improved significantly due to the use of small time steps and non-linear spring-dashpot model at the impacts phase period. The results proved that TBS joint has benefits on decreasing the impacts caused by the clearance.

In this thesis, the main objective is to study the dynamic behavior of four-bar mechanism with clearance in its joint. First, a spring is added to the system in order to reduce the effect of impacts in the joint with clearance. Then the flexibility of the links is used to modify the dynamic behavior of the system. Experimental and analytical results will be used to assess the flexibility on the dynamic behavior of the system.

Chapter 3: Dynamic Behavior of a Four-Bar Mechanism with Clearance and Spring

In this chapter, the description of the dynamic modeling of the four-bar mechanism is presented. Moreover, the modeling of the clearance is discussed and the improvement of the dynamic behavior after attaching spring is investigated through simulation and experimental tests.

3.1 Mechanism Description

Figure 2 shows the four-bar mechanism with a clearance, *e*, in the revolute joint connecting the coupler to the follower.

where:

L_1 is the length of link 1 (the ground) (mm).

L_2 is the length of link 2 (the crank) (mm).

L_3 is the length of link 3 (the coupler) (mm).

L_4 is the length of link 4 (the follower) (mm).

θ_1 is the angle between link 1 and the x axis (degree).

θ_2 is the angle between the x axis and the crank (degree).

θ_3 is the angle between the crank and the coupler (degree).

θ_4 is the angle between the x axis and the follower (degree).

B_3 and B_4 are the attachment points of the spring on the coupler and the follower, respectively.

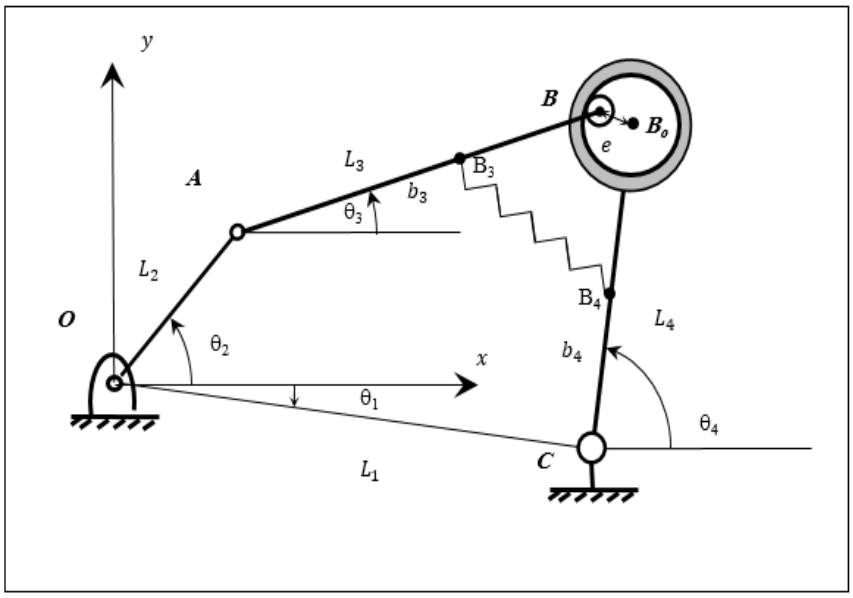

Figure 2: Model of the four-bar mechanism with spring

The four-bar mechanism is made of a rigid crank, a coupler and a rocking follower. The crank rotates at a constant angular velocity of 277 rpm. The geometric and inertia parameters of the mechanism are listed in Table 1.

Table 1: Mechanism parameters

	The ground (1)	The crank (2)	The coupler (3)	The follower (4)
Geometry (mm)	$L_1 = 410$	$L_2 = 100$	$L_3 = 380$	$L_4 = 256$
Mass (kg)		$m_2 = 1$	$m_3 = 0.284$	$m_4 = 0.106$
Inertia (Kg. m^2)		$I_2 = 0.0023$	$I_3 = 35 \times 10^{-3}$	$I_3 = 6 \times 10^{-3}$
Center of mass		$r_{g2} = 0$	$r_{g3} = L_3/2$	$r_{g4} = L_4/2$
Spring	Stiffness k Unstreched length of s_0		$AB_3 = b_3$	$CB_4 = b_4$

3.2 Four-Bar Mechanism Dynamic Modeling

From Figure 2, the kinematic model of the 4-bar mechanism is derived from the literature [28] as follow:

Loop Closer Equation:

$$OA + AB = OC + CB \tag{1}$$

$$L_2 e^{i\theta} + L_3 e^{i\theta} = L_1 e^{i\theta} + L_4 e^{i\theta} \tag{2}$$

$$L_2 Cos\theta_2 + L_3 Cos\theta_3 = L_1 Cos\theta_1 + L_4 Cos\theta_4 \tag{3}$$

$$L_2 \sin\theta_2 + L_3 \sin\theta_3 = L_1 \sin\theta_1 + L_4 \sin\theta_4 \tag{4}$$

Let: $L_1 = R_1$, $L_2 = R_2$, $L_3 = R_3$, and $L_4 = R_4$

Using equations (2) and (3) to calculate θ_3 and θ_4 as follow:

$$\theta_4 = 2\,arctan\left(\frac{-B \pm \sqrt{B^2 - 4AC}}{2A}\right) \tag{5}$$

Repeat the steps to find θ_3 :

$$\theta_3 = 2\,arctan\left(\frac{-E \pm \sqrt{E^2 - 4DF}}{2D}\right) \tag{6}$$

where:

$$D = \cos\theta_2 - K_1 - K_4\cos\theta_2 + K_5 \tag{7}$$

$$E = -2\sin\theta_2 \tag{8}$$

$$F = K_1 - (K_4 - 1)\cos\theta_2 + K_5 \tag{9}$$

Finding the dynamic responses of the mechanism (position, velocity and acceleration):

The position (θ):

$$R_2\cos\theta_2 - R_4\cos\theta_4 = -R_3\cos\theta_3 + R_1\cos\theta_1 \tag{10}$$

$$R_2\sin\theta_2 - R_4\sin\theta_4 = -R_3\sin\theta_3 + R_1\sin\theta_1 \tag{11}$$

The velocity ($\dot{\theta}$)

$$R_2\dot{\theta}_2\sin\theta_2 - R_4\dot{\theta}_4\sin\theta_4 = -R_3\dot{\theta}_3\sin\theta_3 - R_1\dot{\theta}_1\sin\theta_1 \tag{12}$$

$$R_2\dot{\Theta}_2\cos\theta_2 - R_4\dot{\theta}_4\cos\theta_4 = -R_3\dot{\theta}_3\cos\theta_3 + R_1\dot{\theta}_1\cos\theta_1 \tag{13}$$

The acceleration ($\ddot{\theta}$):

$$R_2\dot{\theta}_2^{\,2}\cos\theta_2 - R_4\ddot{\theta}_4\sin\theta_4 - R_4\dot{\theta}_4^{\,2}\cos\theta_4 = -R_3\ddot{\theta}_3\sin\theta_3 - R_3\dot{\theta}_3^{\,2}\cos\theta_3 \tag{14}$$

$$-R_2\dot{\theta}_2^{\,2}\sin\theta_2 - R_4\ddot{\Theta}_4\cos\theta_4 - R_4\dot{\theta}_4^{\,2}\cos\theta_4 = -R_3\ddot{\theta}_3\sin\theta_3 + R_3\dot{\theta}_3^{\,2}\sin\theta_3 \tag{15}$$

Kinestatic model:

Newton's law, which is applied to the three-moving links, yields 9 equations with 9 unknowns, which are the 8 reaction forces and the input torque. The following set of linear equations is solved to obtain these unknowns:

$$\begin{bmatrix} 1 & 0 & 1 & 0 & 0 & 0 & 0 & 0 & 0 \\ 0 & 1 & 0 & 1 & 0 & 0 & 0 & 0 & 0 \\ 0 & 0 & L_2\sin\theta_2 & -L_2\cos\theta_2 & 0 & 0 & 0 & 0 & 1 \\ 0 & 0 & -1 & 0 & 1 & 0 & 0 & 0 & 0 \\ 0 & 0 & 0 & -1 & 0 & 1 & 0 & 0 & 0 \\ 0 & 0 & -r_2\sin\theta_3 & r_3\cos\theta_3 & -(L_3-r_3)\sin\theta_3 & -(L_3-r_3)\cos\theta_3 & 0 & 0 & 0 \\ 0 & 0 & 0 & 0 & -1 & 0 & 1 & 0 & 0 \\ 0 & 0 & 0 & 0 & 0 & -1 & 0 & 1 & 0 \\ 0 & 0 & 0 & 0 & L_4 Sin\theta_4 & -L_4 Cos\theta_4 & 0 & 0 & 0 \end{bmatrix} * \begin{bmatrix} R_{12}^x \\ R_{12}^y \\ R_{32}^x \\ R_{32}^y \\ R_{43}^x \\ R_{43}^y \\ R_{14}^x \\ R_{14}^y \\ T_2 \end{bmatrix} = \begin{bmatrix} m_2 a^x{}_{G_2} \\ m_2 a_{G_2}^y \\ (I_2 + m_2 r_2^2)\ddot{\theta}_4 \\ m_3 a_{G_3}^x - F_{S3}^X \\ m_3 a_{G_3}^y - F_{S3}^Y \\ I_3\ddot{\theta} - T_{S3} \\ m_4 a_{G_4}^x + F_{S4}^X \\ m_4 a_{G_4}^y + F_{S4}^Y \\ (I_4 + m_4 r_4^2)\ddot{\theta}_4 - T_{S4} \end{bmatrix}$$

where:

$a_{G_2}, a_{G_3}, a_{G_4}$ are the accelerations of the center of gravity for links 2, 3 and 4, respectively.

Spring force calculation:

$$F_S = k(S - S_o)e^{i\alpha_S} \tag{16}$$

$$\theta_S = a\tan 2\left(\frac{B_3B_4{}^y}{B_3B_4{}^x}\right) \tag{17}$$

S_o is the free length of the spring

3.3 Clearance Modeling

The clearance in the revolute joint connecting the coupler to the follower is modeled by the introduction of two additional degrees of freedom; the horizontal and the vertical displacements, *x* and *y*, of the journal center relative to the sleeve center (Figure 3). The journal diameter is 7 mm while the sleeve inner diameter is 8 mm.

During the contact, the interaction between the two parts in the joint is only carried out by the normal and the tangential forces of contact. The kinematic contact condition for a revolute joint with radial clearance *e* and relative displacements, *x* and *y*, is given by:

$$g = e - \sqrt{x^2 + y^2} \le 0 \tag{18}$$

The situation where the contact is lost corresponds to $g > 0$ (Figure 3), whereas the contact with local deformation, referred to as a penetration, corresponds to $g < 0$.

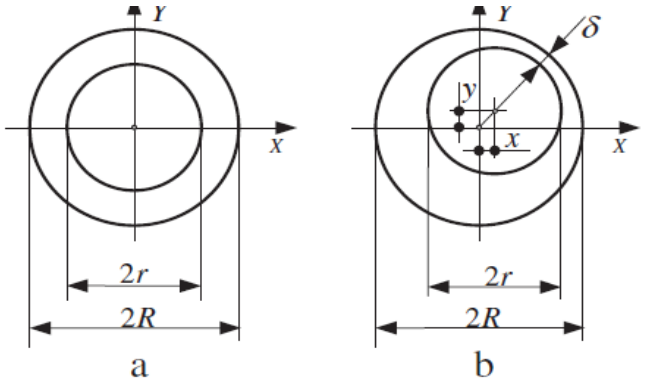

Figure 3: (a) ideal revolute joint, (b) realistic revolute joint [13]

To be able to explain the effect of possible impacts, the reaction force between link 3 (coupler) and link 4 (follower), $\boldsymbol{R_{34}}$ should be monitored. If the direction of reaction $\boldsymbol{R_{34}}$ is oriented in the right direction this means the journal and bearing are in the contact phase. However, when the direction changes, it leads to a contact loss which is a consequence of an impact of the journal against the sleeve on the side of the initial contact.

Figure 4 (a) shows the reaction force $\boldsymbol{R_{34}}$ which maintains the contact in point *H*, where, the surface of contact is always normal to the reaction force. This side of contact is sustained as long as the direction of the force $\boldsymbol{R_{34}}$ tempts a positive moment around *A*. On the other hand, Figure 4 (b) shows the direction changes due to the dynamic of the overall system, resulting of negative moment around point *A*, which corresponds to a loss of the contact and the journal ejecting of the other side of the sleeve. Therefore, the direction of the reaction force $\boldsymbol{R_{34}}$ indicates the contact between journal and sleeve condition.

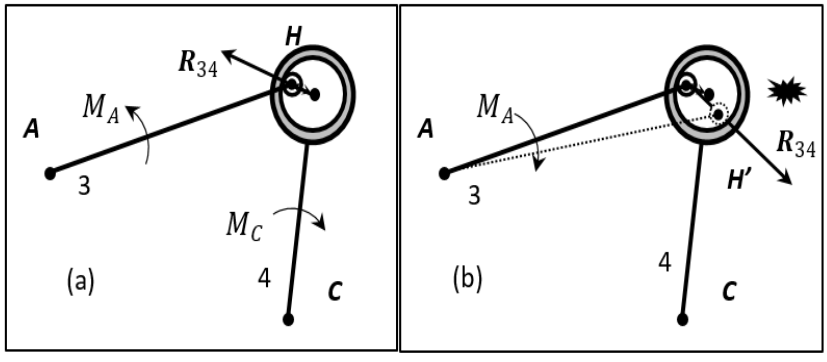

Figure 4: The direction of the reaction force R_34 (a) at an instant t and (b) at t+dt

Thus, to eliminate any impact in the joint with clearance, one has to maintain that the sign of the moment M_A is always the same. The proposed solution is to add a spring to the system to ensure that the contact is maintained at all times.

3.4 Simulation Results

In this section, the simulations of a four-bar mechanism, showed in Figure 2, will be carried out. All the links are considered as rigid and all the joints are without clearance. Following the experimentation, a sampling time of $t = 0.244\ ms$, is used in the simulation. An index is defined representing the number of time steps. This index corresponds to a step of $d\theta_2 = 0.4°$ in the crank rotation, for a speed of $\omega_2 = 29\ rad/s$.

The angular velocity of the crank is assumed to be constant during the motion. Only inertia forces and the input torque are applied to the system. The dynamic model presented results are; the angular velocity of link 3 and link 4 (Figure 5), the angular acceleration of link 3 and link 4 (Figure 6) and the input torque applied to the crank (Link 2), (Figure 7). All these parameters are calculated as a function of the input angle and are shown in the figures below as a function of the index defined above.

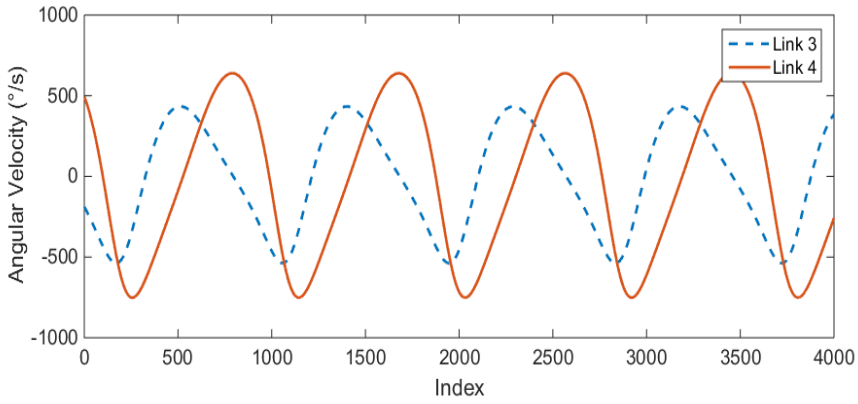

Figure 5: Angular velocity of the coupler (3) and the follower (4)

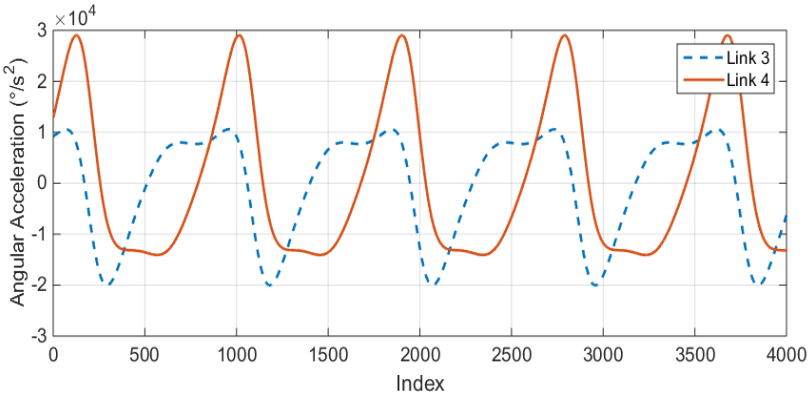

Figure 6: Angular acceleration of the coupler (3) and the follower (4)

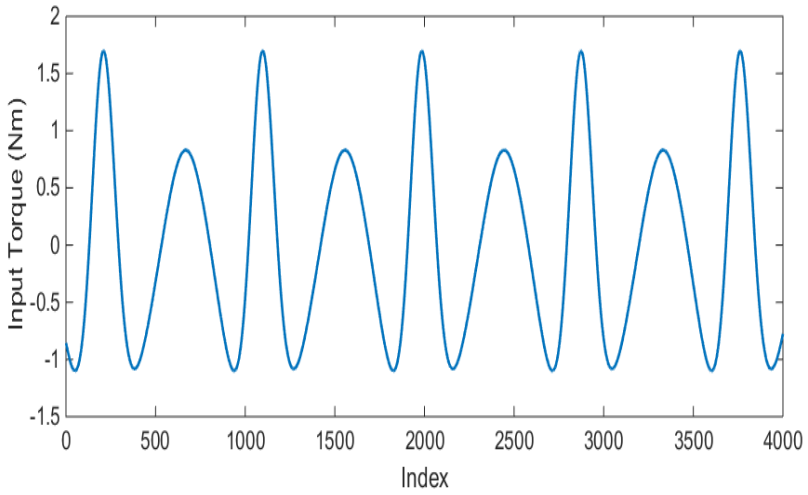

Figure 7: Input torque applied to the crank

Figure 8 shows a simulation of the mechanism where a vector representing the reaction force, $\boldsymbol{R_{34}}$, is shown in each position which can be noticed as the change of reaction forces.

Figure 9 shows the deviation of the moment of the reaction force in the joint around point A, where $\boldsymbol{M_A = AB \times R_{34}}$. It is good to mention that the value of the moment M_A changes sign twice during one rotation of the crank which means two impacts per revolution.

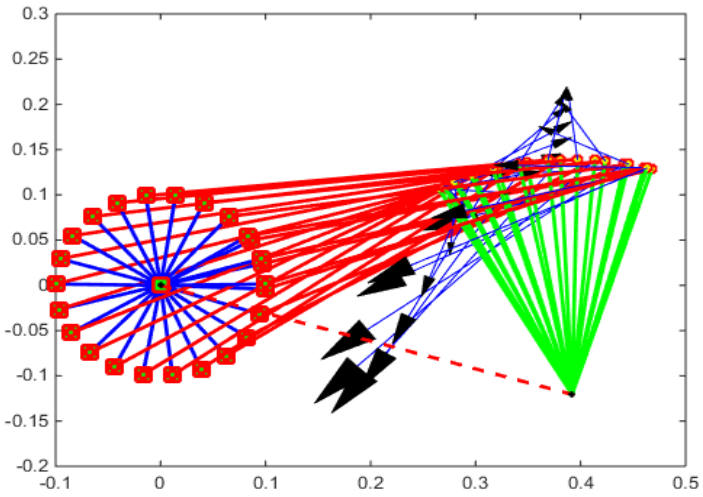

Figure 8: Simulation of the four-bar mechanism showing the vector R_34 in each position

Figure 10 shows the mechanism for three values of the input angle. The first one A^1 associates to the instant just before the impact, the second one at the instant of impact A^2 and the third one A^3 just after the impact.

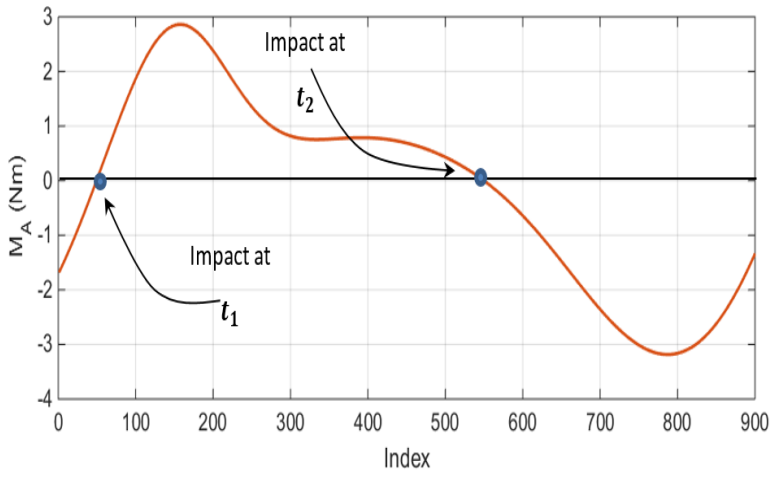

Figure 9: Moment of the reaction force around point A

The reaction force $\boldsymbol{R_{34}}$ is also plotted for these three configurations. The sign of the moment $\boldsymbol{M_A}$ is determined by the relative position of the reaction force $\boldsymbol{R_{34}}$ with respect to link 3. In the configuration in the middle, the reaction is about to change sides and hence the moment is going through zero. At this moment, the contact between the journal and the sleeve in joint B is lost and the journal is going to be ejected against the other side of the sleeve due to the change of sign of the moment $\boldsymbol{M_A}$ on link 3. This change generates a brief impact between the sleeve and the journal, causing the acceleration of any point on link 3 and link 4 to surge to a high value.

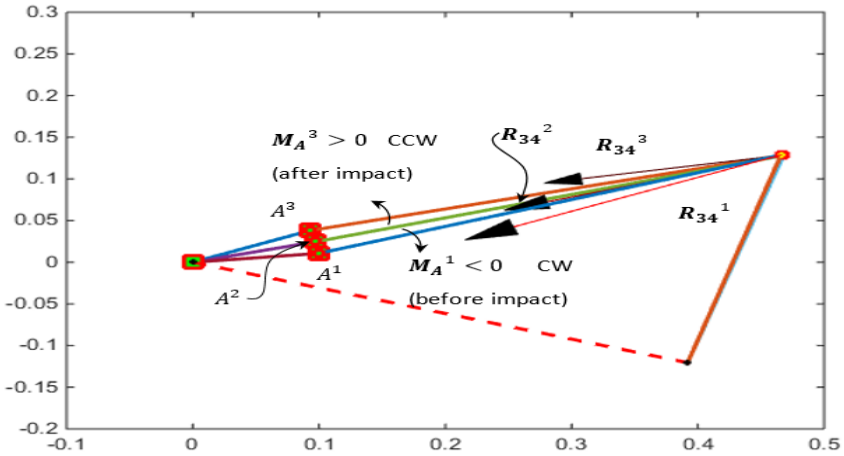

Figure 10: Configurations of the mechanism around the instant of the change of the sign of M_A from a positive value to a negative value (instant t_1 from Figure 9)

Figure 11 shows the second appearance of the change of sign during a full rotation of the crank, which has the same remarks, made for Figure 10. The difference, however, is in the change of direction of the moment $\boldsymbol{M_A}$, which is in the opposite direction compared to prior case. In this case, also, it is noticeable that, the reaction

force has smaller magnitude, which in fact should predict a smaller peak in the acceleration.

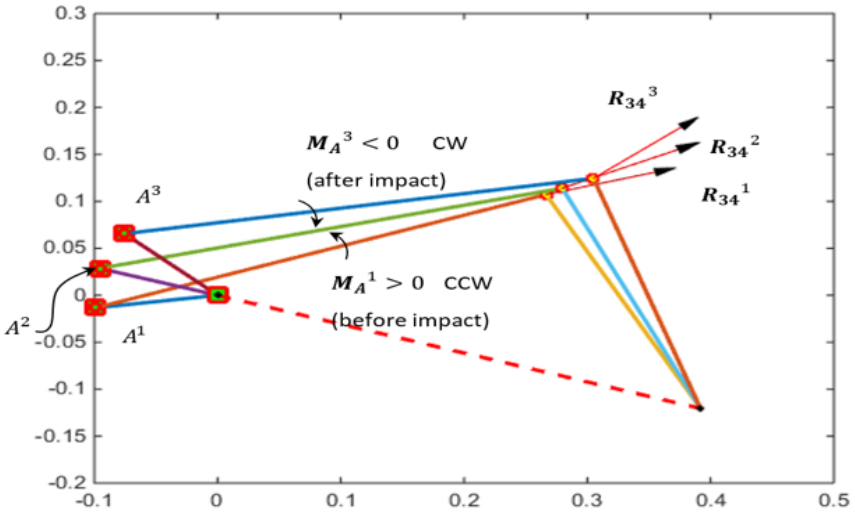

Figure 11: Configurations of the mechanism around the instant of the change of the sign of M_A from a negative value to a positive value (instant t_2 from Figure 9)

3.5 Experimental Setup

In order to validate the simulation results based on the model presented previously, an experimental setup was designed. It consists of a four-bar mechanism driven by a DC motor. The mechanism was first drawn using Auto-desk Inventor software (Figure 12). Then, experimental setup based on the drawing was built by adding a spring as shown in Figure 13.

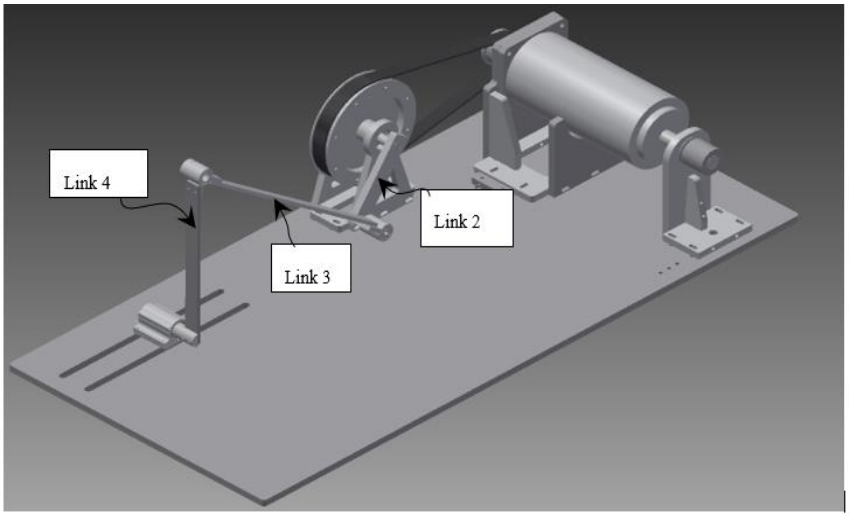

Figure 12: Mechanism model in Auto-desk inventor

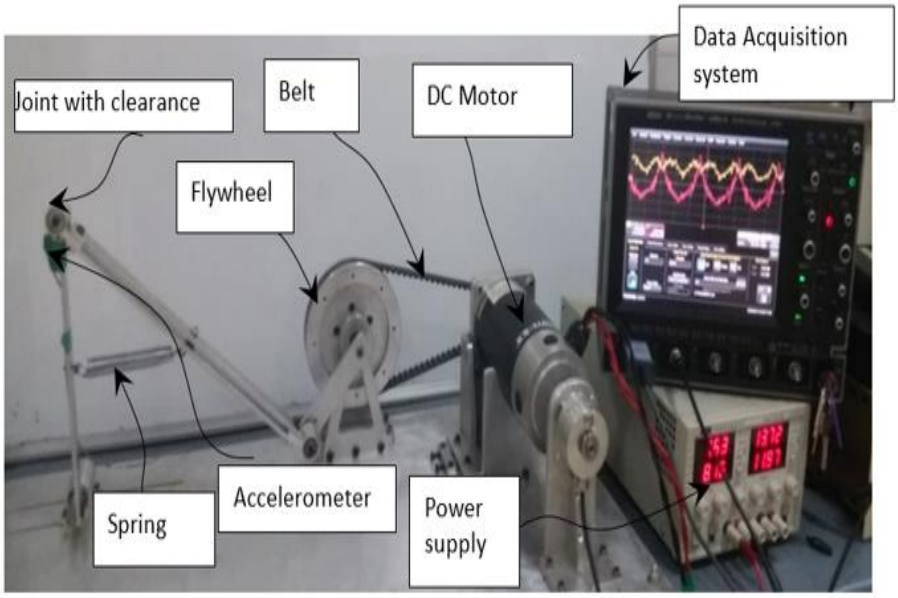

Figure 13: Experimental setup with spring and data acquisition

The revolute joint connecting the coupler to the follower includes a clearance of 1 mm. This exaggerated clearance of 1 mm is selected to emphasize the effect of the impact and permit an easy measurement of the effect of the impact.

A data acquisition system made out of an accelerometer, a tachometer, and a current sensor, was used. The tachometer is used to measure the speed of the motor. The rotation of the crank is ensured, through a pulley pair having a transmission ratio of 3, by a variable speed D.C. permanent magnet servo motor (by MAGMOTOR model: C/S 40 Z2 500) having the following characteristics: Power $P_m = 500\,W$, voltage $V = 24\,V$ and a maximum speed $N = 2700\,rpm$.

A flywheel, having a moment of inertia of 0.026 kg/m², is attached in order to reduce the speed fluctuation of the input link. The accelerometer is used to measure the acceleration near the joint with clearance. All these measurements are made simultaneously during one second of motion, which yields 4098 samples at a sampling time of $t_s = 0.244\,ms$.

The simulation was carried out using MATLAB. The experimental validation is made through the measurement of the acceleration near the joint with clearance. Figure 14 and Figure 15 show a comparison between the simulation and experimental results, in both cases, without and with clearance, respectively, of point D for a crank speed of 277 rpm and one second of acquisition.

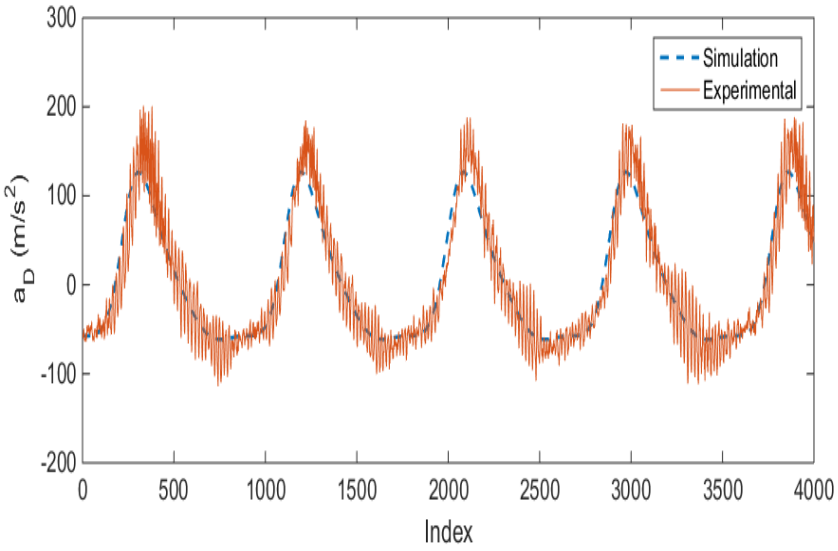

Figure 14: Experimental and analytical results of the acceleration in the case without clearance

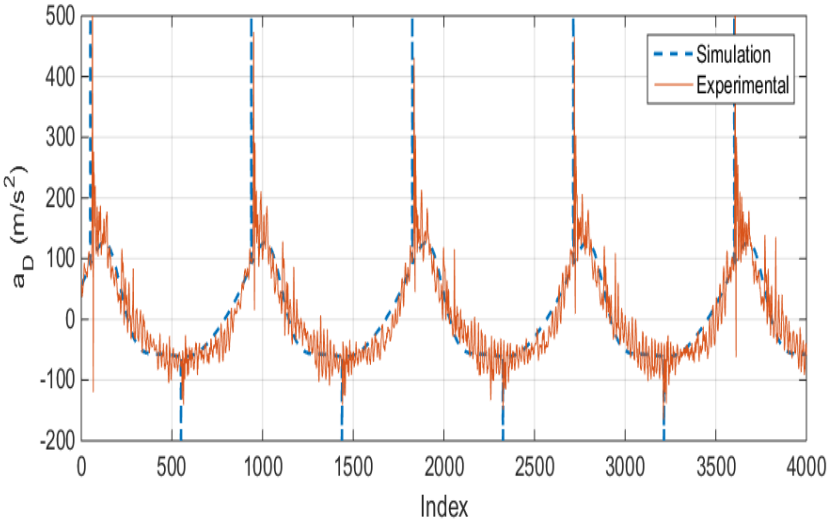

Figure 15: Experimental and simulation results in case with clearance

It is shown that the simulation can predict the presence of the impact by monitoring the reaction force in the joint with clearance. It is important to mention that the value of the acceleration at the instant of impact is not predicted by the simulation. Yet, by comparing the values of the reaction forces shown on Figure 10 and Figure 11, one can see that the higher values of the reaction force occur at the time t_1, which could give an explanation of the higher peak of the acceleration recorded at this instant, compared to the second impact. Since the objective here is to identify the cause of the impact, the results presented in Figure 9 and Figure 15 show clearly that there is a close correlation between the change of the direction of the moment of the reaction force around point A (Figure 2) and the occurrence of the impact.

3.6 Four-Bar Mechanism with a Spring

To be able to reduce the effect of the clearance on the dynamic behavior of the mechanism, the work in [29] proposed adding a second actuator to keep a permanent contact in the joint with clearance. This solution was shown to be effective, but it is too complicated and expensive to implement. In the current work a simple solution, based on the use of springs, is proposed. Since the loss of the contact in the joint with clearance is caused by the changing sides of reaction force R_{34} relative to the coupler link, an added spring can avoid this change and hence yield a permanent contact in the joint with clearance. However, adding a spring requires an extra amount of torque to drive the mechanism. Thus, an optimization of the stiffness of the spring to be implemented and its location has to be defined, in order to minimize the value of the added torque while maximizing the reduction of the impact. In this section, an analysis of the effect of adding a spring to the system is analyzed.

The mechanism now has a spring attached between the coupler and the follower (Figure 2 and Figure 13). The objective is to find the best position of a spring having a stiffness of $k = 279\ N/m$ to keep the moment M_A from changing sign. Figure 16 shows the value of the reaction of the moment of R_{34} around point A, M_A. The presence of the spring resulted in an increase of the mean value of the moment, which can be considered as a negative effect. When the spring is attached in the middle of the two links (curve 2), the moment still has change in signs, which means that the reaction force changes direction in the joint with clearance. However, in the case where the spring is attached in a different location (curve 3), the sign of the moment M_A is kept negative during the motion, which means that no impact is occurring in the joint with clearance.

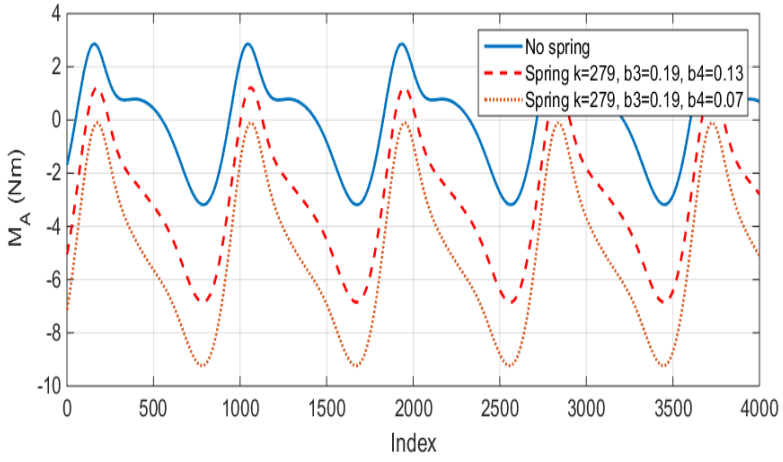

Figure 16: Moment around point A of the reaction force, with and without a spring

As it was mentioned before, the spring has an effect on the input torque required to drive the system. Figure 17 shows that the values of the input torque in the three discussed cases. When the spring is attached in the middle of the two links (curve 2), the simulations show that the input torque increases compared to the case without a spring. However, when the same spring is attached in different positions on the two links (curve 3), the values of the input torque increases but the moment M_A keeps the same sign, as shown in Figure 16 and Figure 17.

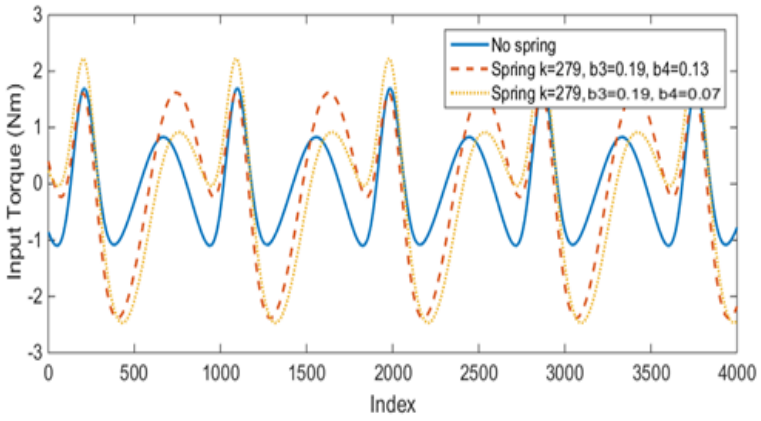

Figure 17: Input torque with and without a spring

Therefore, the spring has positive and negative effects on the dynamic behavior of the system. The objective then is to optimize the parameters of the spring to be added, in order to maximize their benefits while minimizing the negative effect.

Spring Parameters Optimization

In order to find the best values of the parameters of the spring, an optimization technique is implemented. These parameters are defined as attachment points of the spring, k, b_3 and b_4 (Figure 1). The stiffness of the spring is taken as $k = 279\ N/m$ and its pre-tension, represented by the unstretched length, is $s_0 = 110\ mm$.

The objective function used to minimize the peak values of the torque. An optimization method, based on the MATLAB function "GA", is developed. The optimization problem can be formulated as follows:

Objective function:

$$F = \min(T_{max})\ \ (over\ a\ full\ cycle)$$

Subject to the following constrains:

$$0 < b_3 < L_3$$
$$0 < b_4 < L_4$$
$$M_A \leq 0$$

The optimum parameters are found to be: $b_3 = 0.362\,m$, $b_4 = 0.031\,m$. The required input torques for this optimum case along with the case when the same spring is attached in the middle of the two links (initial), are shown in Figure 18. Compared to the value of the torque with no spring, the torque corresponding to the optimized solution maintained similar values.

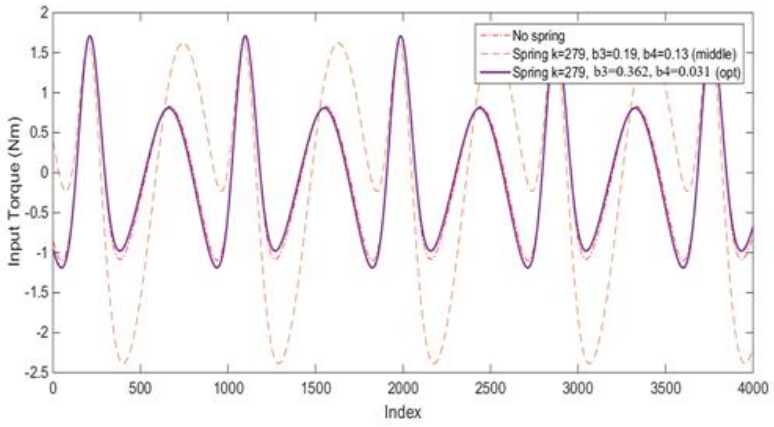

Figure 18: Simulated Input torque for different cases

The measurements shown in Figure 19 are the current drawn by the motor in the three cases used for the simulation. One can notice that the trend of the three curves is similar to the one shown on Figure 18. More investigation of these measurements is, however, needed to correlate the measurements and the simulated results.

Figure 20 shows the evolution of the moment of the reaction force between link 3 and link 4 around point A. When the spring is attached in the middle of the two links, the moment results show change of direction, which will cause impacts during the motion. However, when the same spring is attached at the optimum location given above, the moment keeps the same direction during the motion, which will insure that there will be no impact and the torque values are much less than the prior positions.

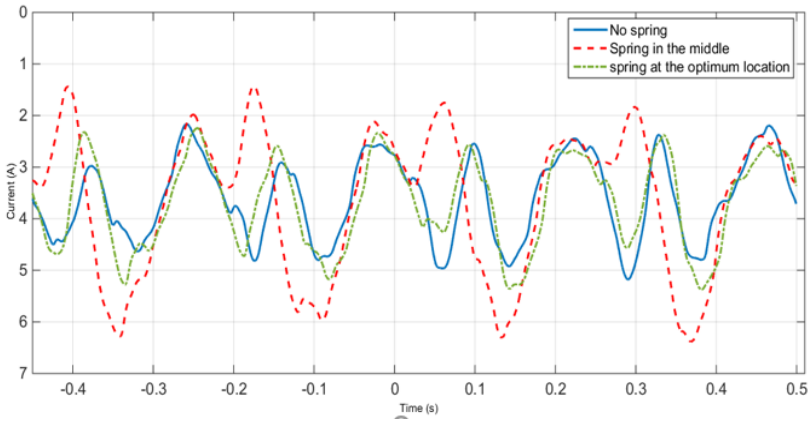

Figure 19: Experimental measurement of the motor current

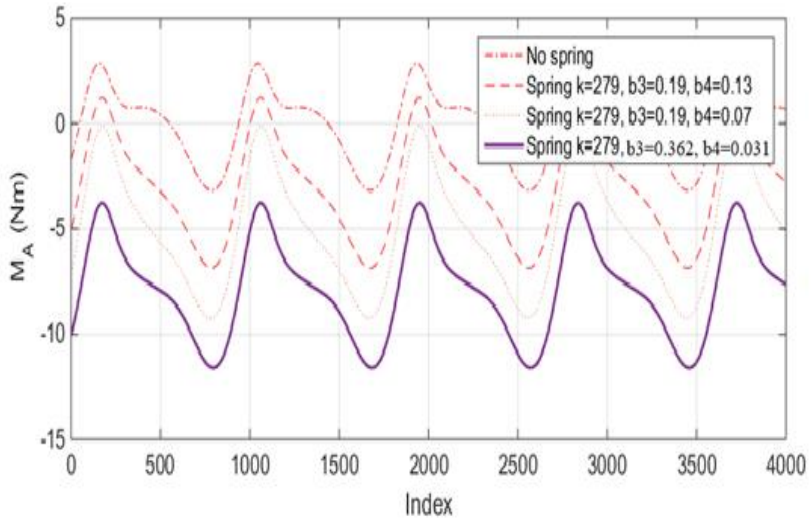

Figure 20: Moment of the reaction force before and after optimization

Experimental results confirm these findings. Figure 21 shows the acceleration in the two above cases, where the impacts are eliminated in case of optimized parameters of spring. Figure 22 obtains the simulation of the mechanism along with the vector representing the reaction force in the joint with clearance, when the spring is attached in its optimum location. It is worth mentioning that, the direction of the reaction force is mostly pointing to the opposite direction compared to the case without a spring (Figure 8). The magnitude, however, is similar to the case without a clearance (Figure 15).

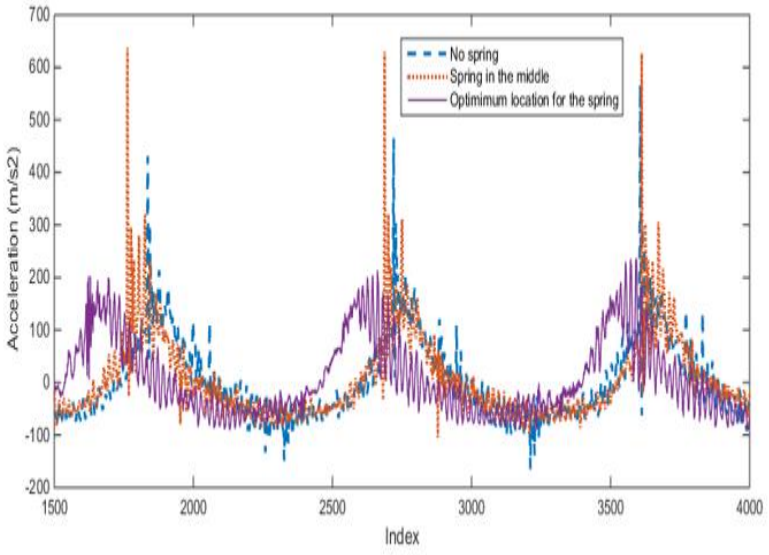

Figure 21: Optimized experimental results

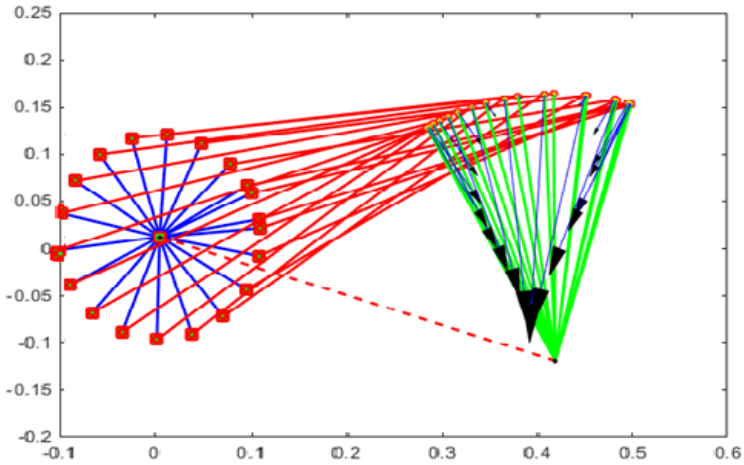

Figure 22: The magnitude and the orientation of the reaction force during the motion

In conclusion, two impacts were predicted by monitoring the moment of the reaction force in the joint with clearance. Adding a spring can keep the reaction force on only one side of link 3, which means no impact in the joint with clearance. Besides, using optimized attachment points of the spring, eliminates the effect of impacts while keeping an acceptable value of the input torque.

Chapter 4: Dynamic Behavior of a Four-Bar Mechanism with Flexible Links

In this chapter, the dynamic behavior of a flexible four bar-mechanism with ideal joints is investigated. The study is done through experimental and simulation tests and the simulation is carried out using ADAMS software. The mechanism has the same characteristics as the one presented in Chapter 3, except that the coupler link is modeled as elastic. In order to have different elasticity characteristics for the coupler link, two different materials with two different thickness values were used as follow:

- Aluminum with thickness values of 3 and 4 mm.
- Steel with thickness values of 1.5 and 2 mm.

4.1 Experimental Setup

The same experimental setup that was used for the rigid case in Chapter 3 is used for the case of flexible mechanism. However, two strain gauges were attached on both sides of each coupler link, in order to measure the elastic deformation. The strain gauges are attached in the middle of the coupler bar to measure the highest value of deformation as it is shown in Figure 23 and Figure 24 . All the coupler bars are cleaned with alcohol before attaching the strain gauge using special type of glue.

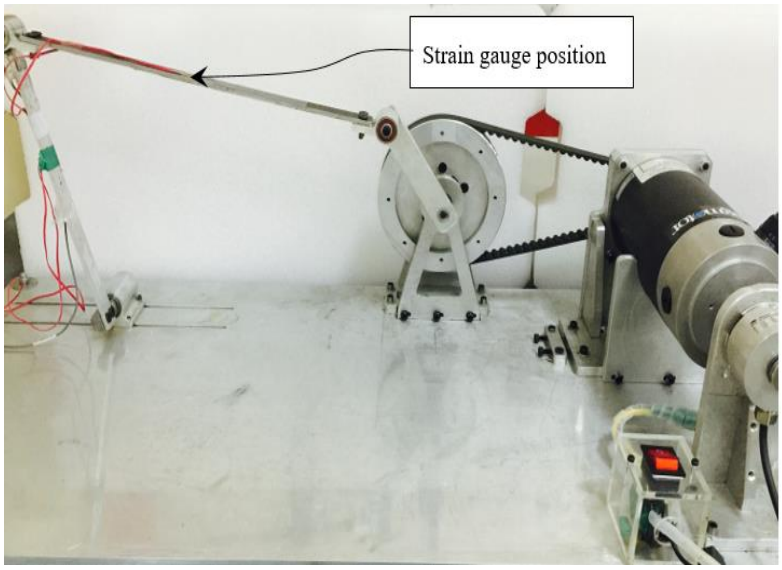

Figure 23: Experimental setup of flexible mechanism with strain gauge

Strain gages are usually used in a bridge configuration with a voltage excitation source in order to measure the strain, which needs accurate measurement of very small changes in resistance.

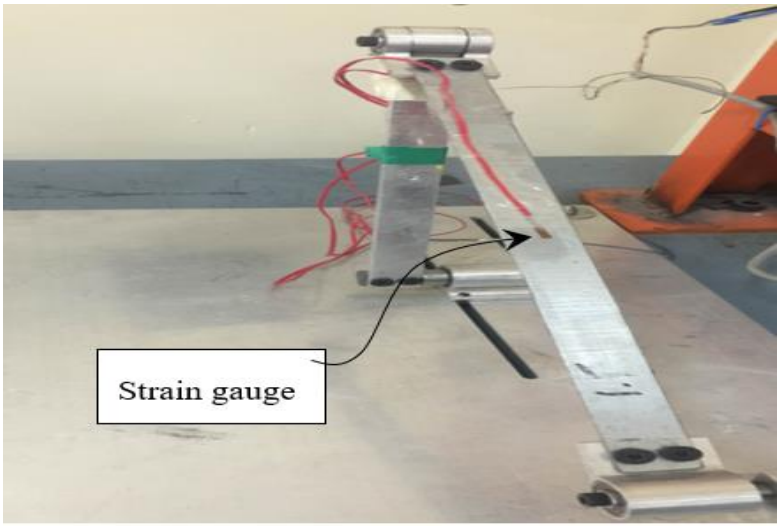

Figure 24: Strain gauge attached to the coupler

The common Wheatstone bridge, showed in Figure 25, includes four resistive arms with an excitation voltage, V_{EX} that is applied across the bridge. The output voltage of the bridge (V_O), is given by the following equation:

$$V_O = \left(\frac{R_3}{R_3 + R_4} - \frac{R_2}{R_1 + R_2} \right) * V_{EX} \tag{19}$$

The bridge is balanced when $R_1 / R_2 = R_4 / R_3$, which results in zero output voltage ($V_O = 0$) and any change in resistance in any arm of the bridge generates a nonzero output voltage. For instance, by replacing R_4 in Figure 25 with an active strain gage, it will unbalance the bridge and provide a nonzero output voltage if any changes in the strain gage resistance occurred [30].

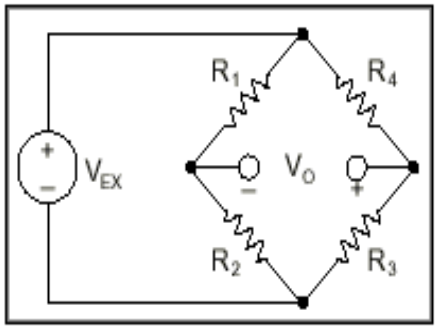

Figure 25: Wheatstone bridge [20]

The sensitivity of the bridge to strain can be doubled by letting both gages active in a half-bridge configuration or it can be increased further by making all four of the

arms of the bridge active strain gages in a full-bridge configuration as shown in Figure 26.

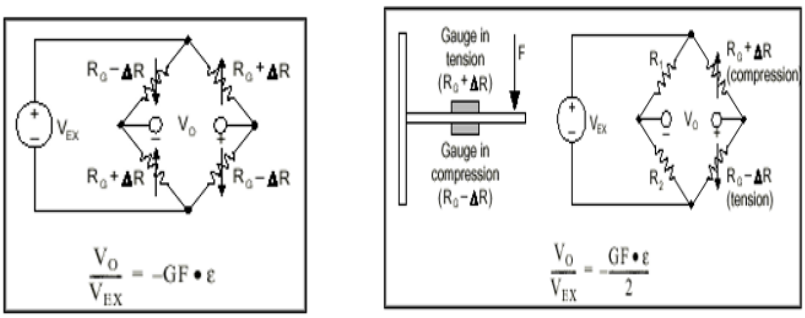

(a) (b)

Figure 26: (a) Full-Bridge Circuit, (b) Half-Bridge Circuit [20]

In the current experimental setup, the half bridge circuit is used where the two strain gauges - attached in both sides of the coupler link- are connected to the Wheatstone bridge with one strain mounted in tension (RG + DR) and the other mounted in compression (RG - DR) side as shown in Figure 26 (b).

Since the resistance changes across the strain gauge bridge are small, an amplifier is considered in the setup, which is connected to a Wheatstone bridge as it is shown in Figure 27. Figure 28 shows the module diagram of the strain gauge, which is connected to the Wheatstone bridge and the signal goes into an amplifier. The output of the amplifier is shown on the screen of the acquisition system (Lecroy).

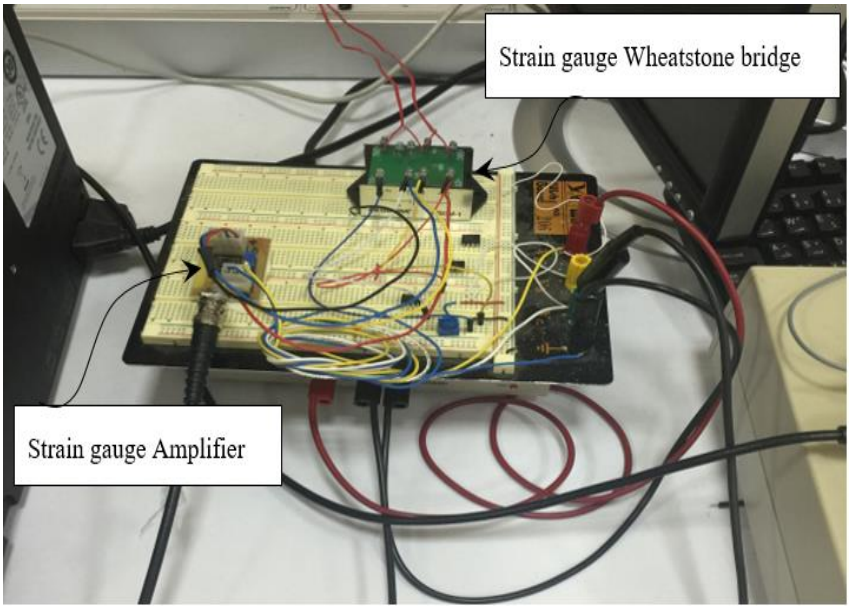

Figure 27: Strain gauge Wheatstone bridge and amplifier

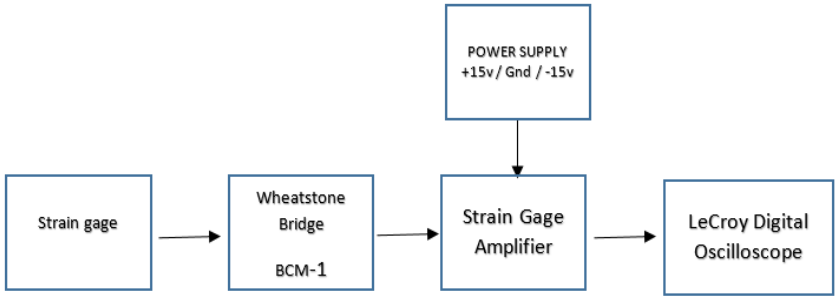

Figure 28: Strain Gage Module Diagram

Figure 29 shows the circuit diagram and PCB layout of the strain gauge amplifier which is built in the lab.

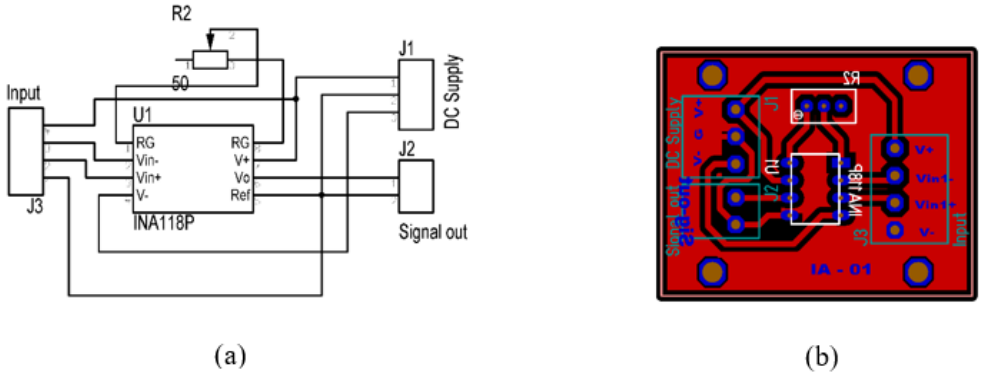

Figure 29: (a) Circuit Diagram of Strain Gauge Amplifier, (b) PCB Layout of Strain Gauge Amplifier

The characteristics of the elastic coupler links are given in Table 2.

Table 2: Flexible coupler links characteristics

The Material	**Aluminum**	**Aluminum**	**Steel**	**Steel**
Thickness	3 mm	4 mm	1.5 mm	2 mm
Mass	0.144 kg	0.163 kg	0.175 kg	0.201 kg
Young Modulus	$6.9 * 10^4\ kPa$	$6.9 * 10^4\ kPa$	$2.07 * 10^5\ kPa$	$2.07 * 10^5\ kPa$

4.1.1 Experimental results. The mechanism was run at three different crank speeds (277 rpm, 415 rpm and 554 rpm) for each of the coupler links defined in Table 2. In this section, the strain values of the flexible coupler are measured and compared

for the three crank speeds in order to compare the deformation of the links according to their materials and thickness values. It is noticeable from Figure 30 (aluminum coupler of 4 mm thickness) that as the speed increases, the strain values increase which are doubled from almost 50 μ strain to 100 μ strain when the speed changed from 277 rpm to 415 rpm, respectively. The strain values increased further as the mechanism is driven at the highest speed 554 rpm to slightly higher than 200 μ strain.

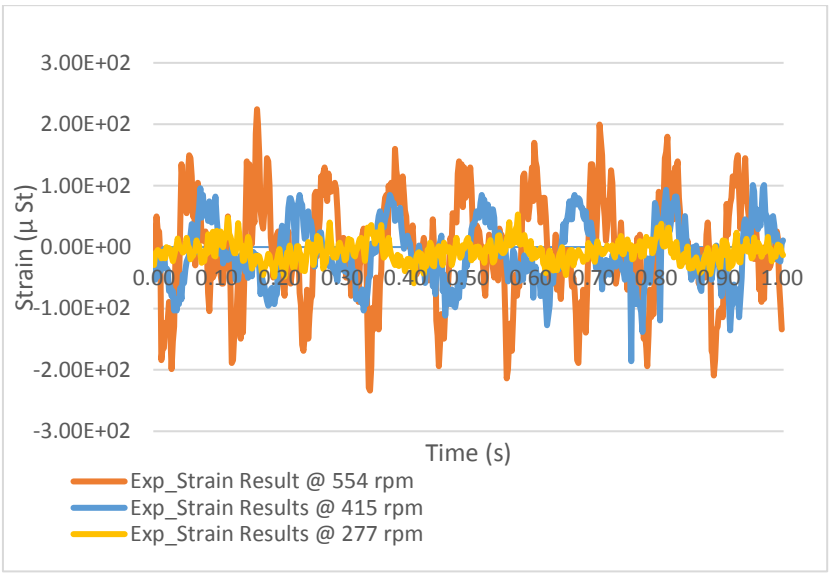

Figure 30: Experimental strain results for Aluminum with 4 mm thickness coupler (three speeds)

For the 3 mm thickness coupler the deformation in the link is greater than the previous case where the highest value is slightly higher than 400 μ strain compared to 200 μ strain of aluminum 4 mm coupler (Figure 30 and Figure 31).

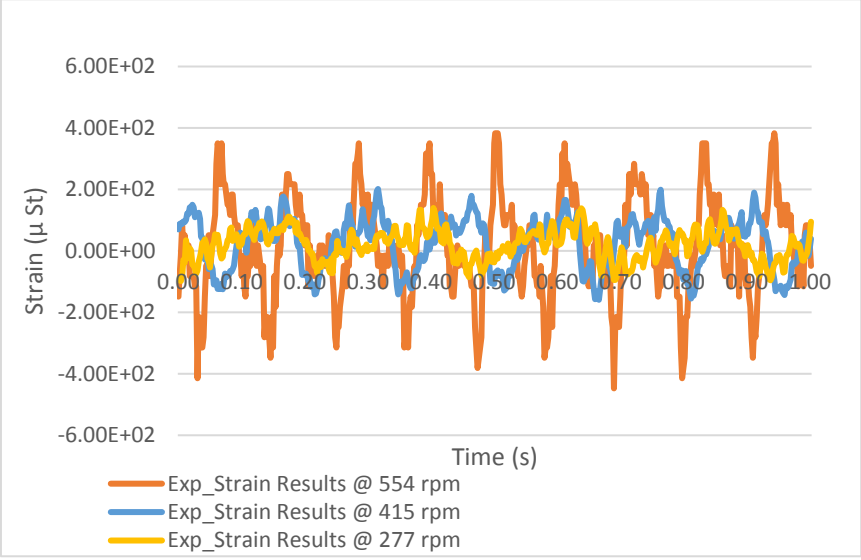

Figure 31: Experimental strain results for Aluminum with 3 mm thickness coupler (three speeds)

It is interesting to remark that the positive and negative values indicate that the bar deforms in both sides (up and down), assuming that the deformation in tension side (downward) gives positive values and for the compression side (upward) results in negative values. Figure 31 to Figure 33 shows that the maximum deformation happened in the compression side (upward) except for aluminum 4 mm, the deformation in both sides has almost the same values, as shown in Figure 30.

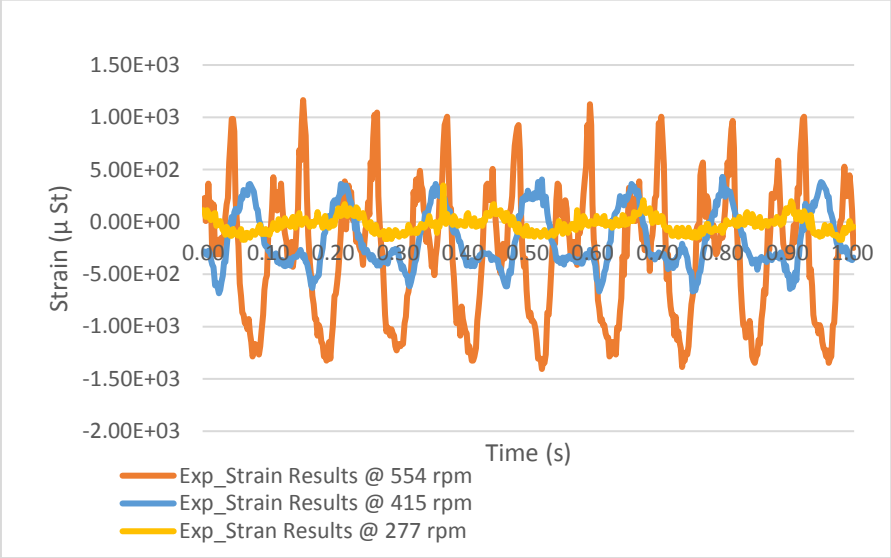

Figure 32: Experimental strain results for Steel with 2 mm thickness coupler (three speeds)

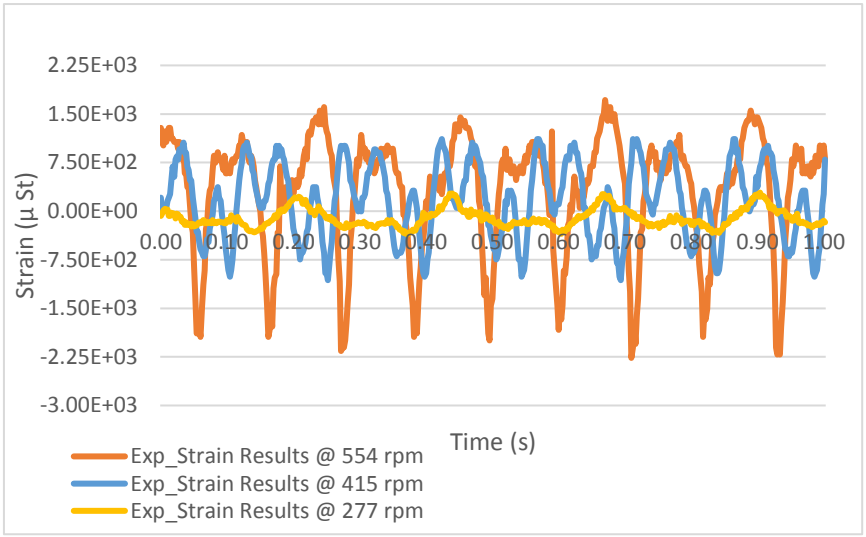

Figure 33: Experimental strain results for Steel with 1.5 mm thickness coupler (three speeds)

The deformation for the steel coupler is increased significantly as it reached 1000 µ strain for the steel with 2 mm thickness and more than 2000 µ strain for steel of 1.5 mm thickness as shown in Figure 32 and Figure 33.

4.2 Simulation Results

The model of the four-bar mechanism was built using ADAMS software in order to validate the experimental results. Except for the coupler link, the dimensions and the materials of the links are the same as the ones used in the rigid mechanism setup in Figure 13.

Figure 34 shows a rigid mechanism and the coupler material is set as steel with 5 mm thickness. The joints that connect the links are defined as revolute joints.

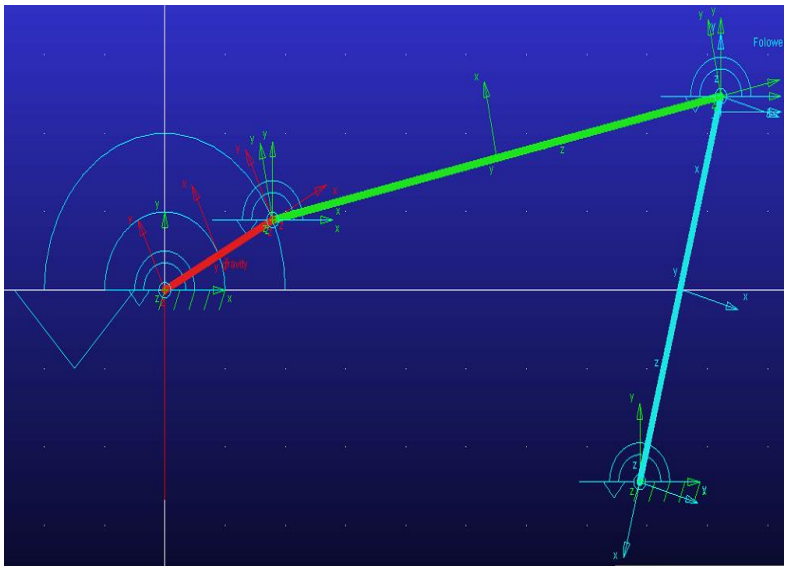

Figure 34: Four-bar mechanism under ADAMS software

In order to make the coupler link flexible, few steps must be considered which can be created under the software itself as shown in Figure 35. The list of steps is:

1- Modify the coupler link with the required thickness, (1.5 mm for example).
2- Choose the number of modes, which is set as 10 because the first six modes in the software are the rigid modes.
3- Select the element type, which set as quadratic in this case.
4- Define the meshing sizes after setting the element specification as size instead of auto.
5- After meshing the bar is completed, the attachments of the link with other links should be defined to complete the creation the flexible link.

Figure 36 displays the first four flexible modes. ADAMS software enables to calculate the eign-frequencies and eigen-modes of the flexible coupler, which are specific to each used bar. The simulation tests were run for each case (depending on the

used coupler links) at three different speeds, i.e., 277 rpm, 415 rpm and 554 rpm. These are the same speeds used in the experimental setup.

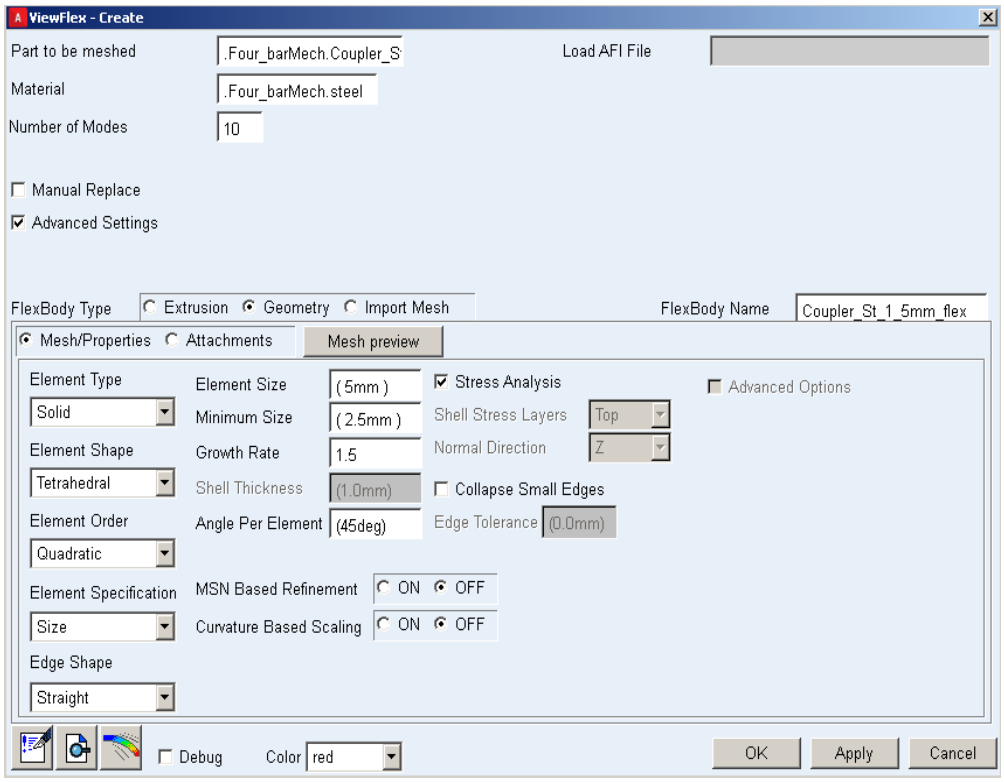

Figure 35: Major steps of making the flexible link

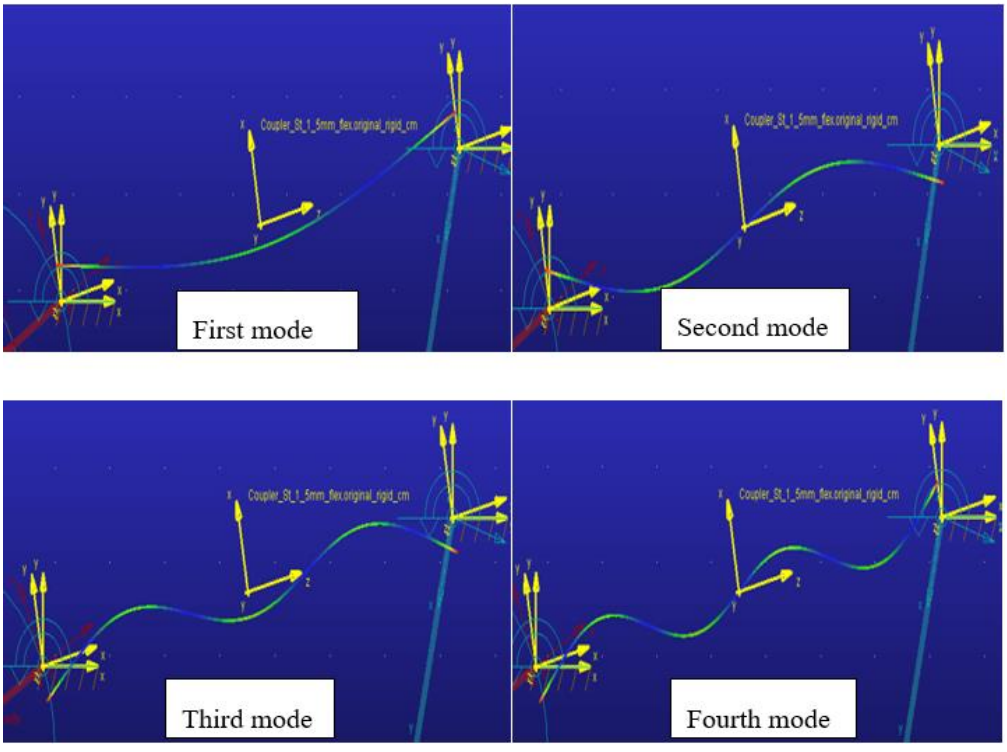

Figure 36: Flexible coupler mode shapes

4.2.1 Aluminum-4 mm thickness. In this section, the simulation and experimental results were compared for the model with aluminum coupler of 4 mm thickness at the three speeds. The strain values of this coupler link of 4 mm is quite small compared to the results of the other coupler links because it has a high stiffness.

It is noticeable from Figure 37-Figure 39 that the simulation and experimental results have the same trends, however, the experimental results have much more fluctuations than the simulation results due to the noise in acquiring the strain signal.

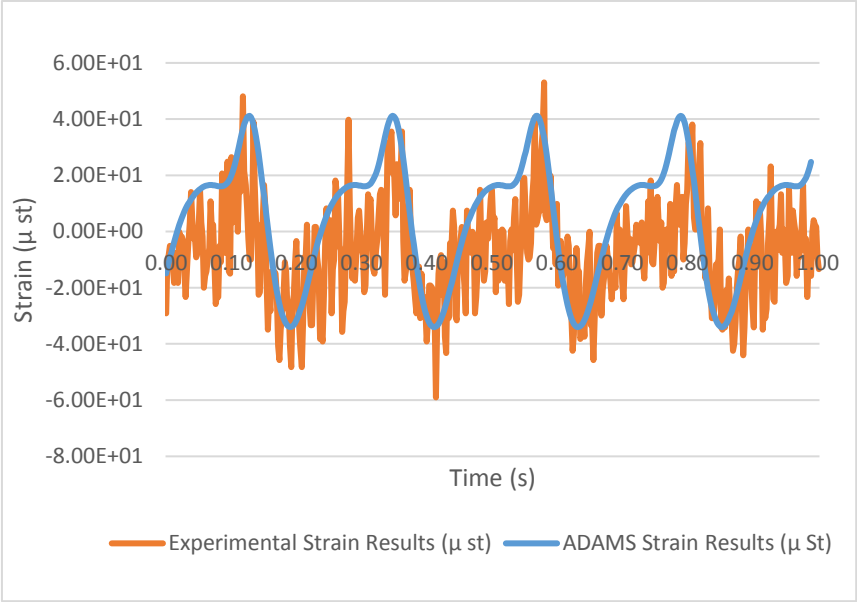

Figure 37: Experimental and simulation strain results for Aluminum (4 mm thickness) at 277 rpm

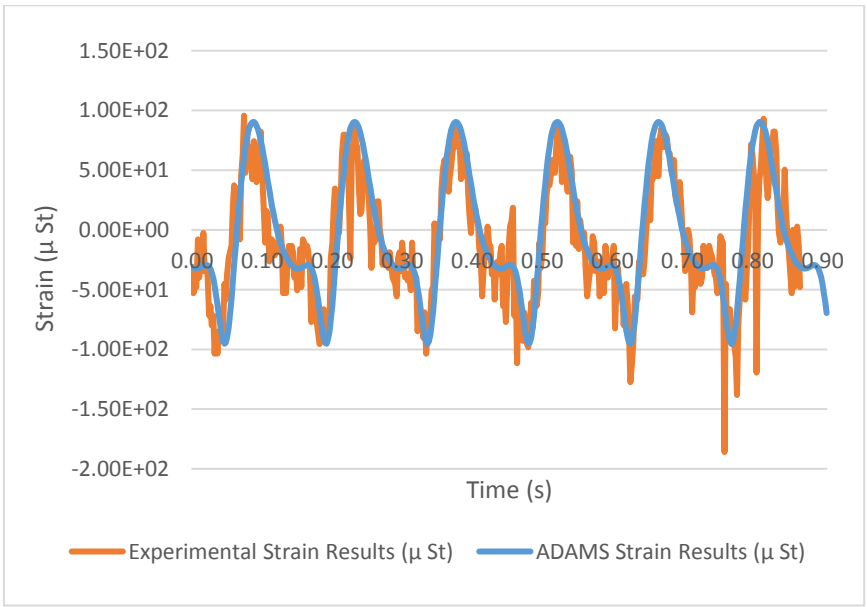

Figure 38: Experimental and simulation strain results for Aluminum (4 mm thickness) at 415 rpm

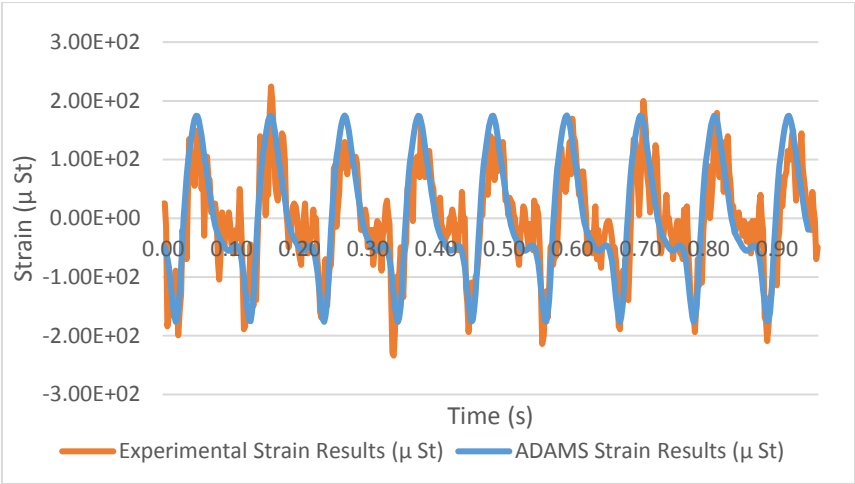

Figure 39: Experimental and simulation strain results for Aluminum (4 mm thickness) at 554 rpm

4.2.2 Aluminum-3 mm thickness. Figure 40 to Figure 42 indicate the experimental and simulation results for the aluminum coupler of three mm thickness. The results indicate that the aluminum has further fluctuations than aluminum with four mm thickness and has higher strain values because it has less stiffness value than the prior.

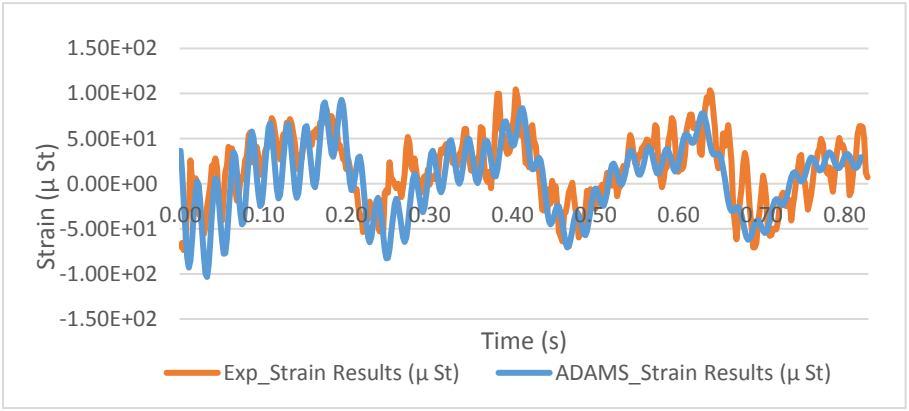

Figure 40: Experimental and simulation strain results for Aluminum (3 mm thickness) at 277 rpm

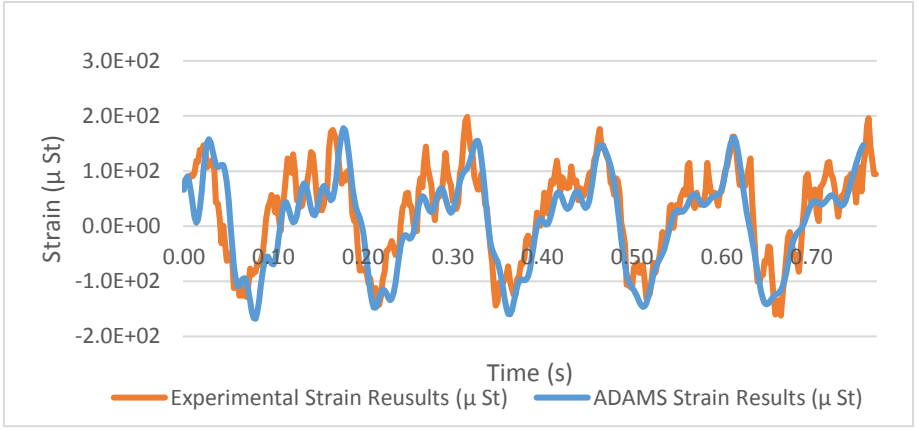

Figure 41: Experimental and simulation strain results for Aluminum (3 mm coupler thickness) 415 rpm

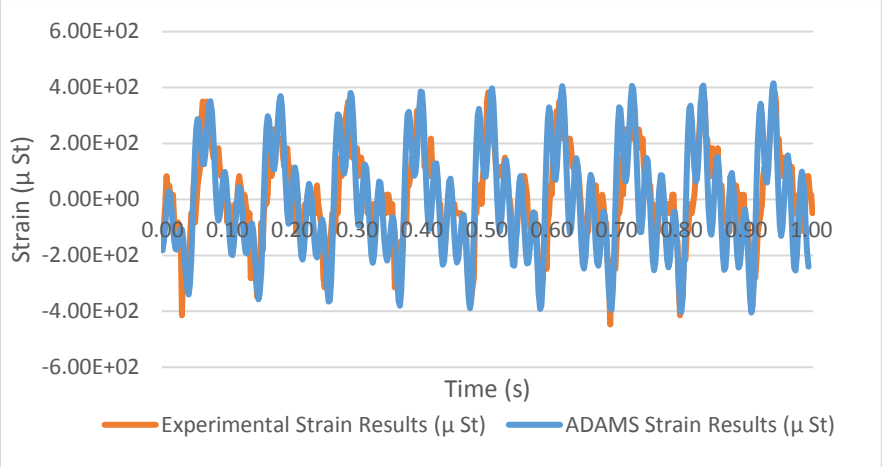

Figure 42: Experimental and simulation strain results for Aluminum (3 mm coupler thickness) 554 rpm

4.2.3 Steel-2 mm thickness. Figure 43, 44 and 45 show the strain results in the case of a coupler in steel with 2 mm thickness for 3 different speeds. It is significant to mention that the results have much less fluctuations than in the case of aluminum with 4 mm and 3 mm. However, it has greater strain values. This means that the steel coupler with 2 mm thickness has higher deformation.

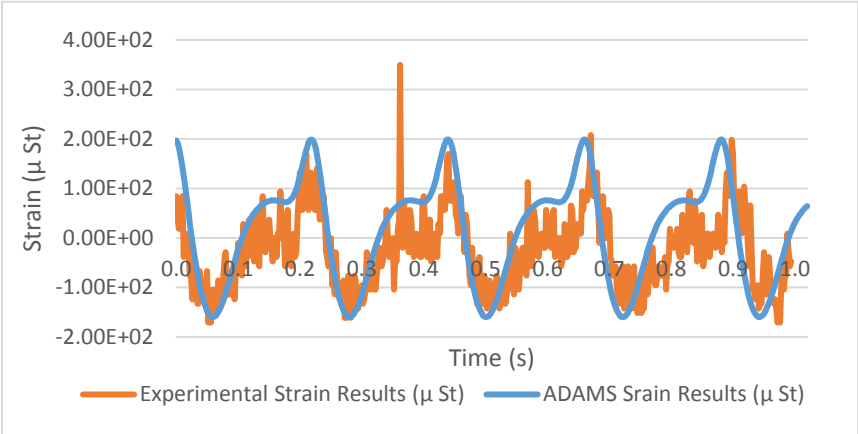

Figure 43: Experimental and simulation strain results for Steel (2 mm thickness) at 277 rpm

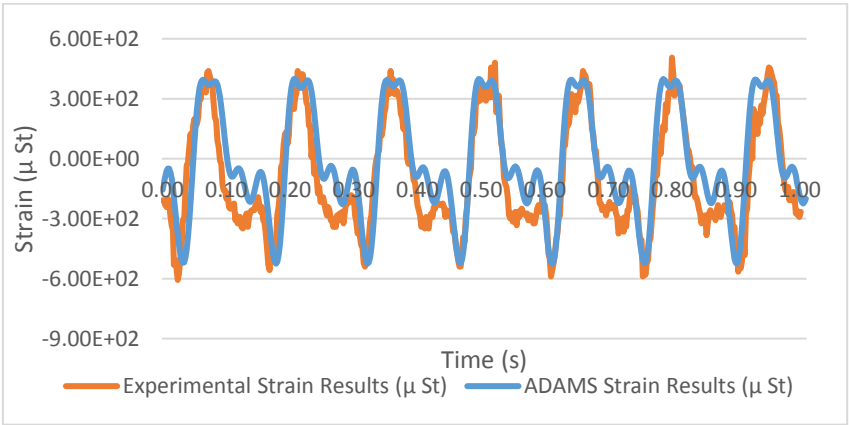

Figure 44: Experimental and simulation strain results for Steel (2 mm thickness) at 415 rpm

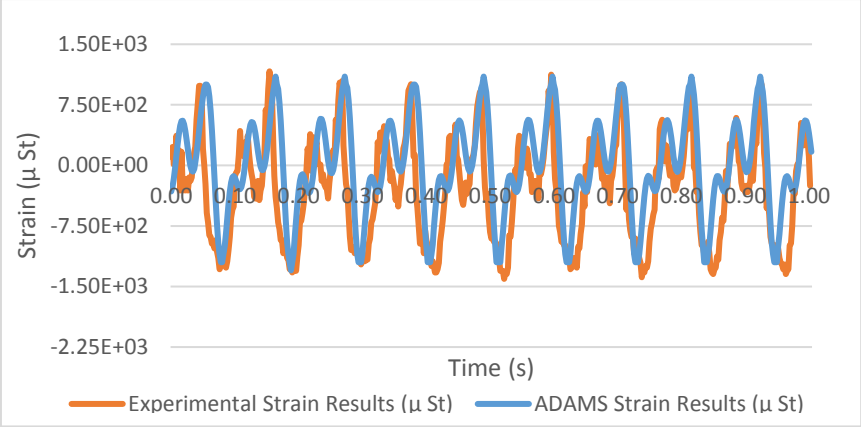

Figure 45: Experimental and simulation strain results for Steel (2 mm thickness) at 554 rpm

4.2.4 Steel-1.5 mm thickness. In case of steel-1.5 mm, Figure 46 to Figure 48 show that the deformation in the bar is nearly a plastic deformation because the thickness is small. Therefore, the results show high values of strain, especially at speed of 554 rpm.

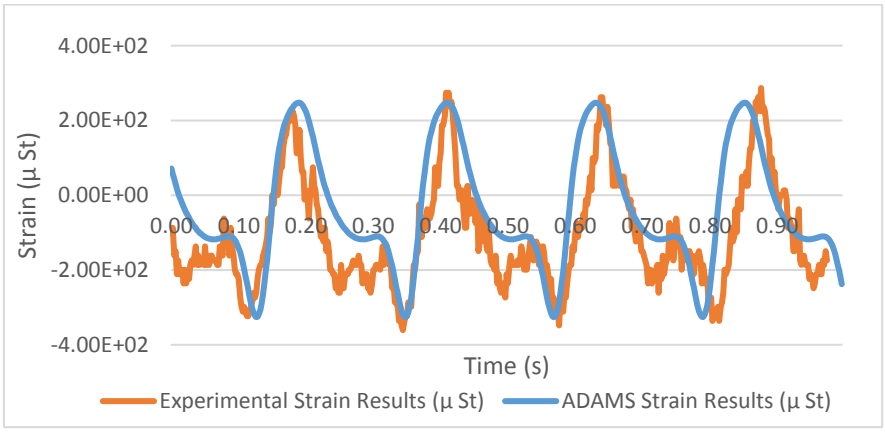

Figure 46: Experimental and simulation strain results for Steel (1.5 mm thickness) at 277 rpm

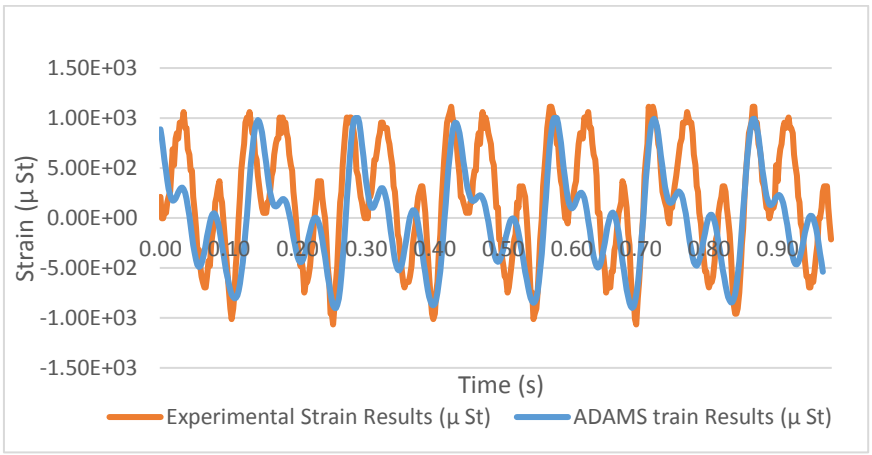

Figure 47: Experimental and simulation strain results for Steel (1.5 mm thickness) at 415 rpm

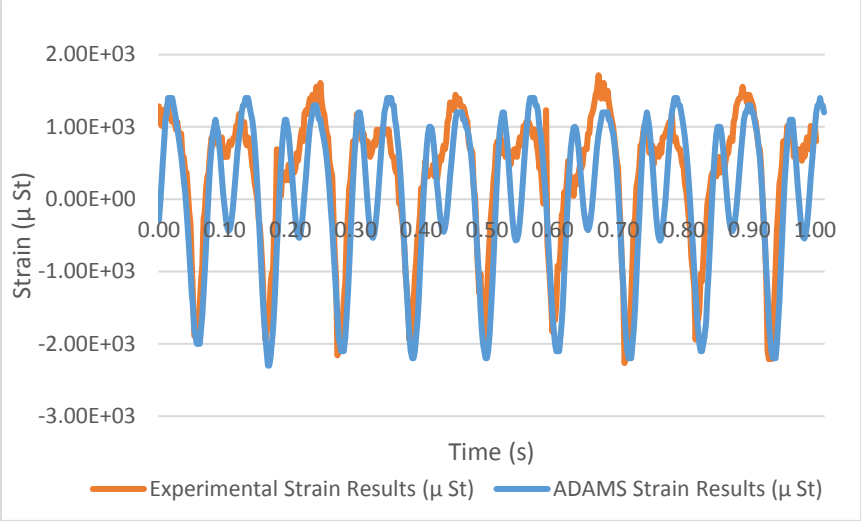

Figure 48: Experimental and simulation strain results for Steel (1.5 mm thickness) at 554 rpm

In conclusion, the deformation of the coupler links was investigated through experiments and validated with simulation tests. The results show a good agreement in most of the cases. It can be noticed from the results that when the speed increases, the strain values rise significantly. Besides, the flexibility of the bar increases as the thickness decreases.

Chapter 5: Dynamic Behavior of a Four-Bar Mechanism with Clearance and Flexible Links

In this chapter, the study of the dynamic behavior of a flexible four bar-mechanism with joint with clearance is performed. The dynamic behavior of the mechanism is investigated for two different sizes of clearance in the joint (0.5 mm and 1 mm) for the same characteristics of the flexible coupler links mentioned in chapter 4. A rigid mechanism with steel coupler of 5 mm is also considered to emphasize the effect of the flexible coupler on the dynamic behavior of the mechanism. The study is carried out through experiments and simulation (ADAMS software).

5.1 Experimental Results

In this section, the acceleration values are measured using an accelerometer, which is attached to the follower link near the joint with clearance (Figure 13). The mechanism was run at three different crank speeds (277 rpm, 415 rpm and 554 rpm) for each one of the coupler links (flexible and rigid).

5.1.1 Rigid case with ideal joints (no clearance). In order to address the effect of the crank speed on the dynamic behavior of the rigid mechanism (steel coupler with 5 mm thickness); the acceleration values are measured at the three mentioned speeds with ideal joints as shown in Figure 49.

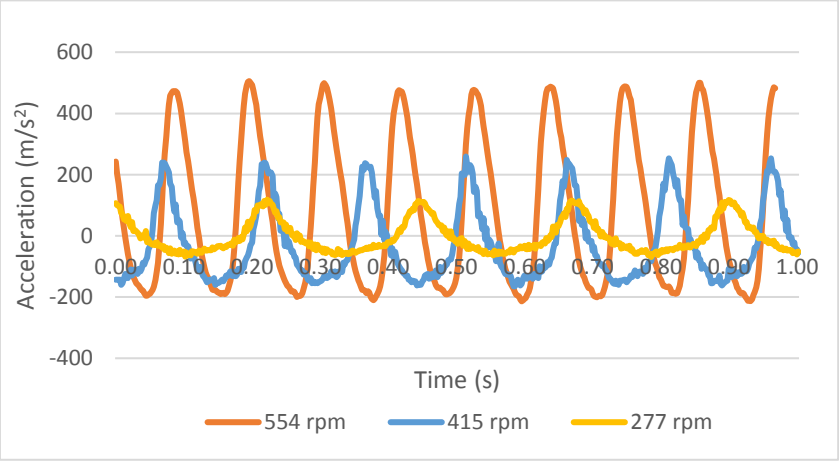

Figure 49: Experimental follower acceleration results for steel-5mm coupler (three speeds)

Figure 49 confirms that, when the speed increases, the acceleration values increases significantly. It can be seen that the acceleration increases from 100 m/s^2 at 277 rpm to 250 m/s^2 at 415 rpm. The acceleration values increased further at the highest speed 554 rpm to 500 m/s^2.

5.1.2 Flexible case with ideal joint (no clearance). In this section, the acceleration values for the different flexible mechanisms (aluminum with 3 and 4 mm thickness values and the steel with 1.5 and 2 mm thickness values for coupler link) are measured at the three defined speeds using ideal joints (Figure 50).

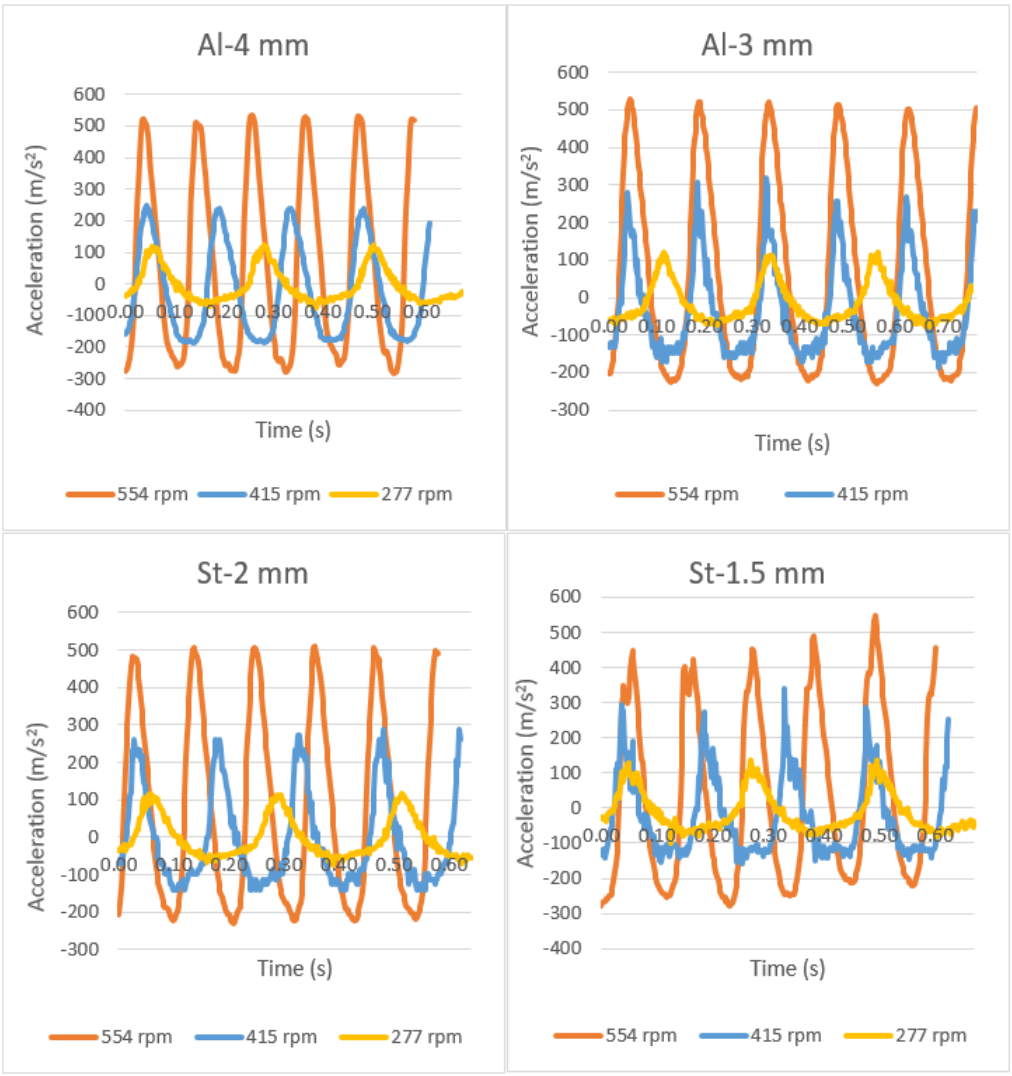

Figure 50: Experimental follower acceleration results for the flexible mechanisms (three speeds)

It can be observed from Figure 50 that the acceleration values for the flexible mechanisms are almost the same as the rigid mechanism. This indicates that the stiffness of the coupler link (thickness) does not affect the system vibration when the joints are ideal.

5.1.3 Rigid case with clearance. In order to emphasize the effect of clearance size on the mechanism, the acceleration results are plotted using two sizes of clearance (0.5 and 1 mm) and ideal mechanism (no clearance) in one figure at the three different crank speeds.

Figure 51 shows the acceleration results of steel with 5 mm thickness for the three clearance sizes at 277 rpm. It can be observed that the size of the clearance in the joint affects the acceleration values considerably.

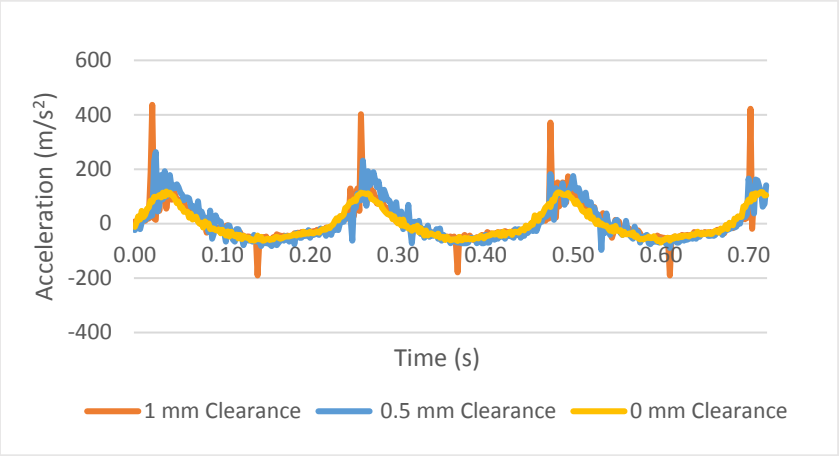

Figure 51: Experimental follower acceleration results for steel-5mm (three clearance sizes) at 277 rpm

It can be noticed that the acceleration rose from 100 m/s^2 for 0 mm clearance to 250 m/s^2 for 0.5 mm clearance to slightly higher than 400 m/s^2 for 1 mm clearance at speed 277 rpm. The situation exacerbated by the higher speed, where the acceleration extremely increased up to 600 m/s^2 and 1000 m/s^2 at 415 rpm for 0.5 mm and 1 mm -clearance sizes- respectively as shown in Figure 52. Whereas, for the highest speed 554 rpm, the values of acceleration reached nearly 1500 m/s^2 for 1 mm clearance in the joint (Figure 53).

It is interesting to mention that for no clearance case, the acceleration values show very smooth results whereas, for 0.5 mm and 1 mm clearance sizes, the results show two peaks per cycle which indicates the occurrence of impacts.

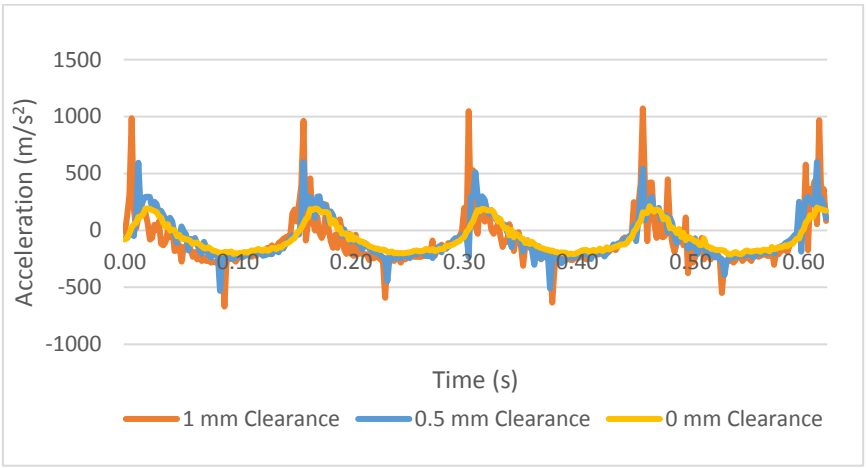

Figure 52: Experimental follower accelerations for steel-5 mm (three clearance sizes) at 415 rpm

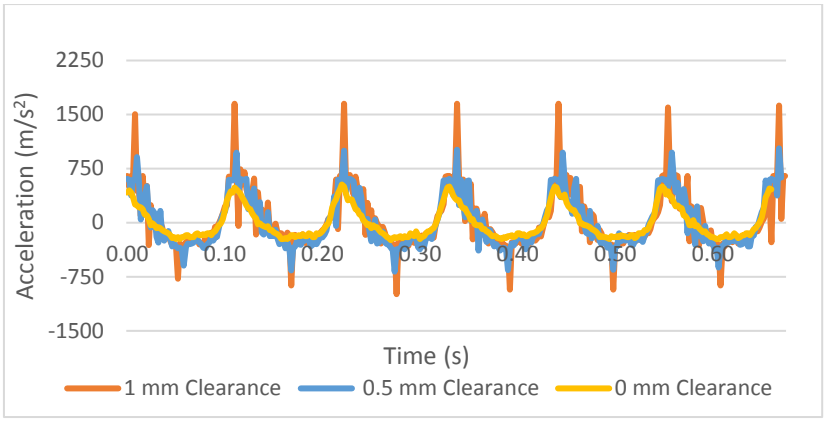

Figure 53: Experimental follower accelerations for steel 5-mm (three clearance sizes) at 554 rpm

5.1.4 Flexible case with clearance. Aluminum-4mm:

Figure 54 shows that using an aluminum coupler with 4 mm thickness provides much better results than the rigid case. As it can be seen, the acceleration results for no clearance and 0.5 mm clearance are almost the same at the three speeds with some small peaks in the case of 0.5 mm clearance. However, for 1 mm clearance the number of peaks increased especially when the speed went up to 415 rpm and 554 rpm.

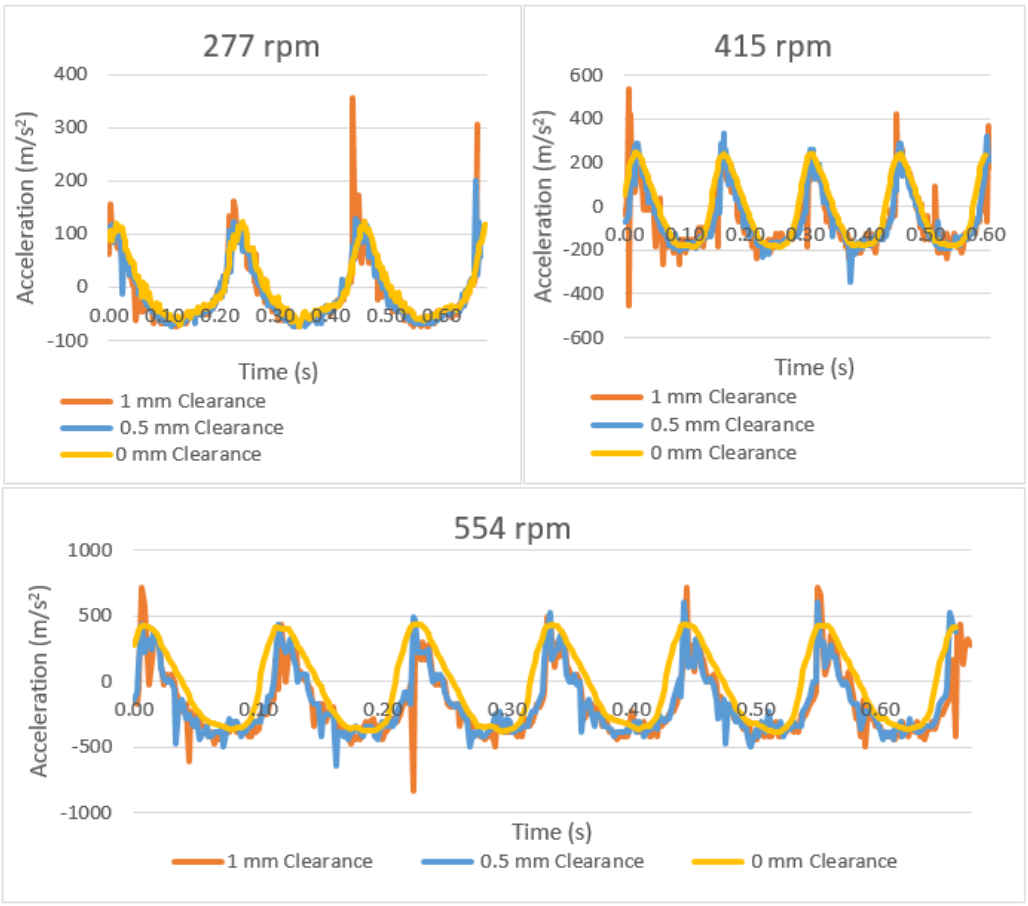

Figure 54: Experimental accelerations for aluminuim-4 mm at three speeds (three clearance sizes)

Alumium-3mm:

For aluminum with 3 mm thickness, it can be observed from Figure 55 that the effect of clearance (0.5 mm and 1 mm) is nearly eliminated at the speed of 277 and the acceleration results show almost the same trends like the ideal joint case. Whereas, at the higher speeds 415 and 554 rpm, the results show small peaks.

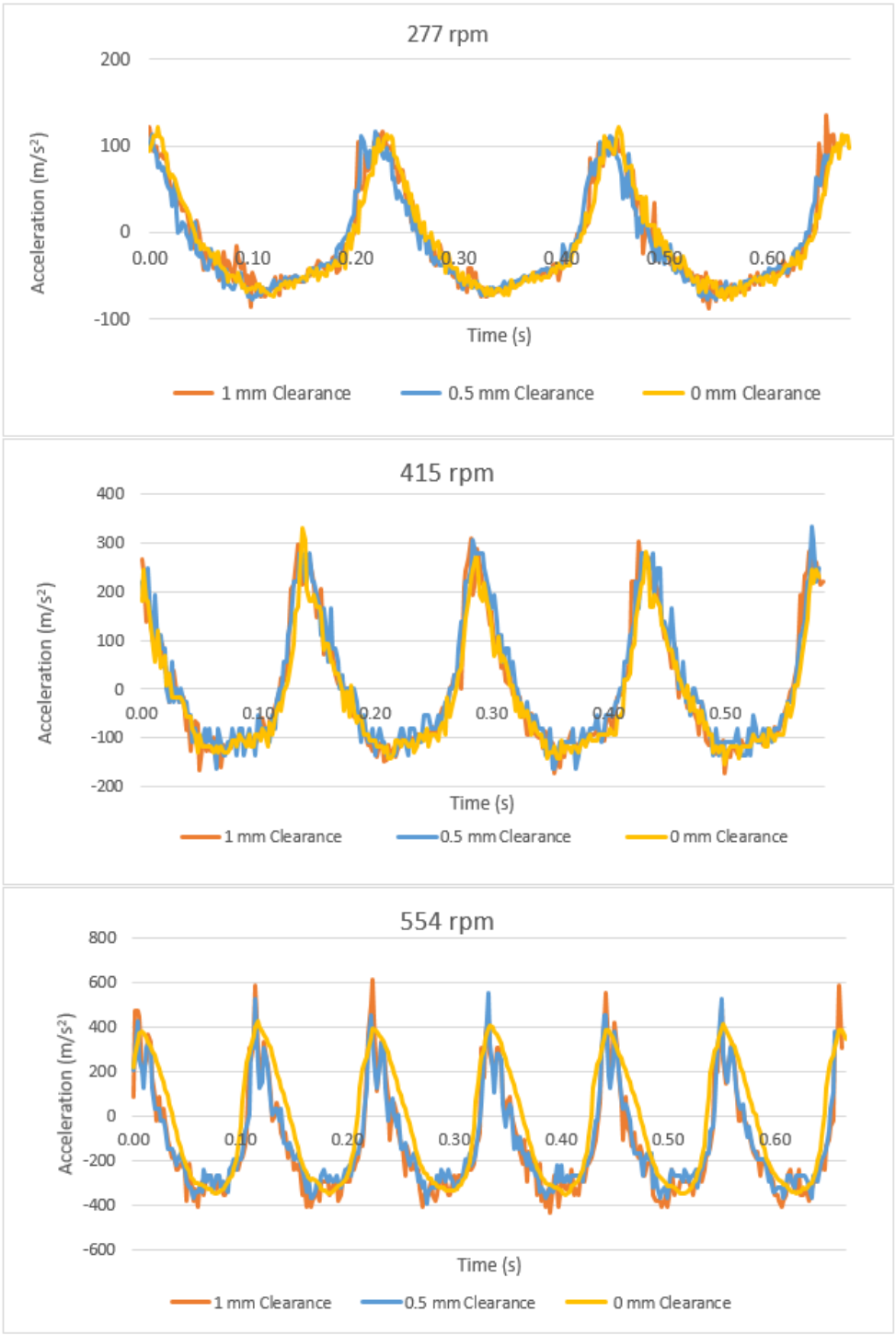

Figure 55: Experimental accelerations for aluminuim-3 mm at three speeds (three clearance sizes)

Steel-2mm:

For steel with 2 mm thickness, the effect of 0.5 mm clearance is trivial compared to the effect of 1 mm clearance where the peaks are almost removed for the case of 0.5 mm clearance as shown in Figure 56. On the other hand, the joint with 1 mm clearance outcomes of small peaks increase when the speed increases.

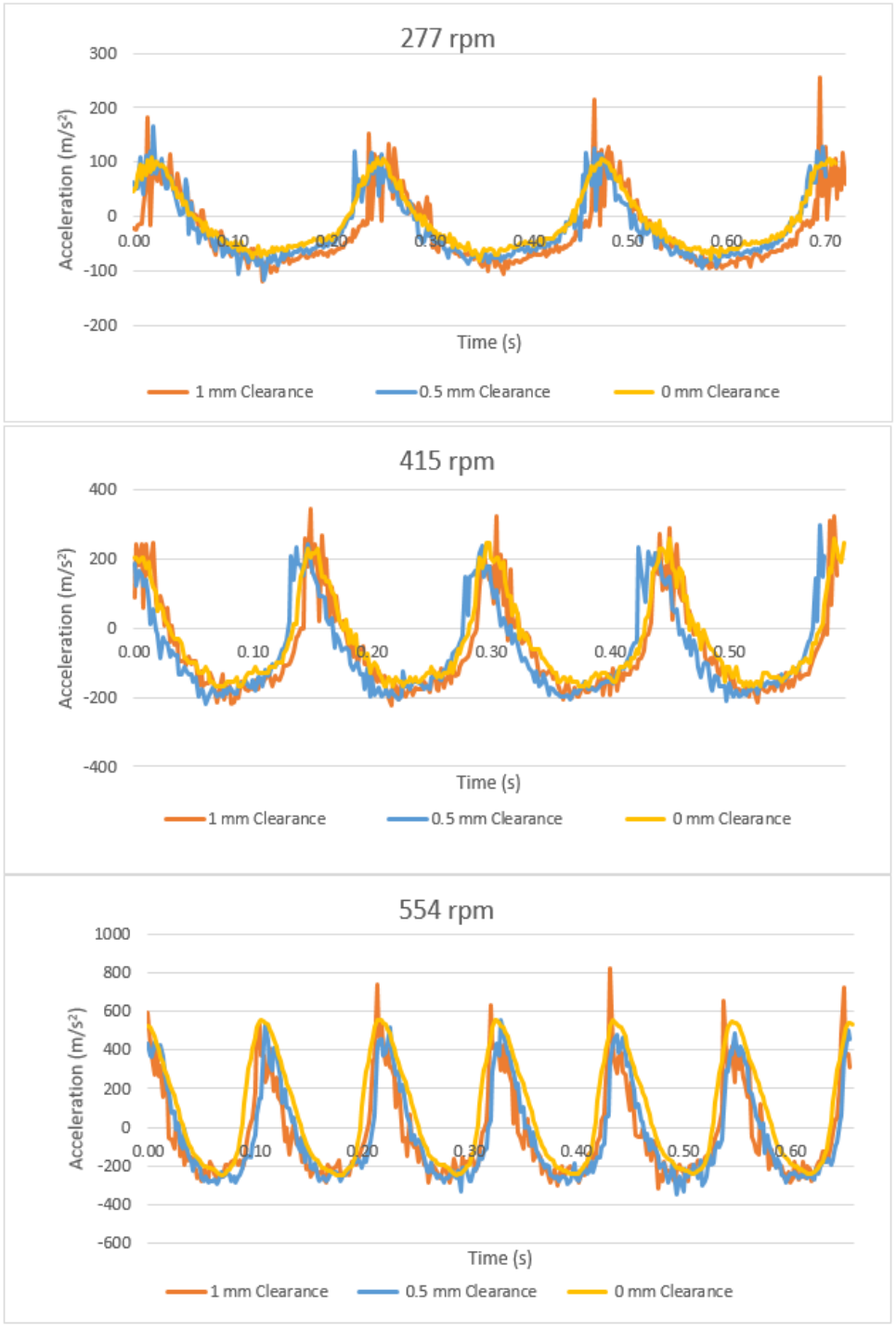

Figure 56: Experimental accelerations for steel-2 mm at three speeds (three clearance sizes)

Steel-1.5mm:

It can be noticed from Figure 57 that the steel with 1.5 mm has more peaks for both cases 0.5 mm and 1 mm clearances compared to the other flexible cases. The acceleration results reached 250 m/s^2 in the case of joint with clearance compared to 100 m/s^2 for the joint with no clearance at 277 rpm, while at higher speeds the acceleration values reached 500 m/s^2 and 800 m/s^2 at 415 rpm and 554 rpm, respectively.

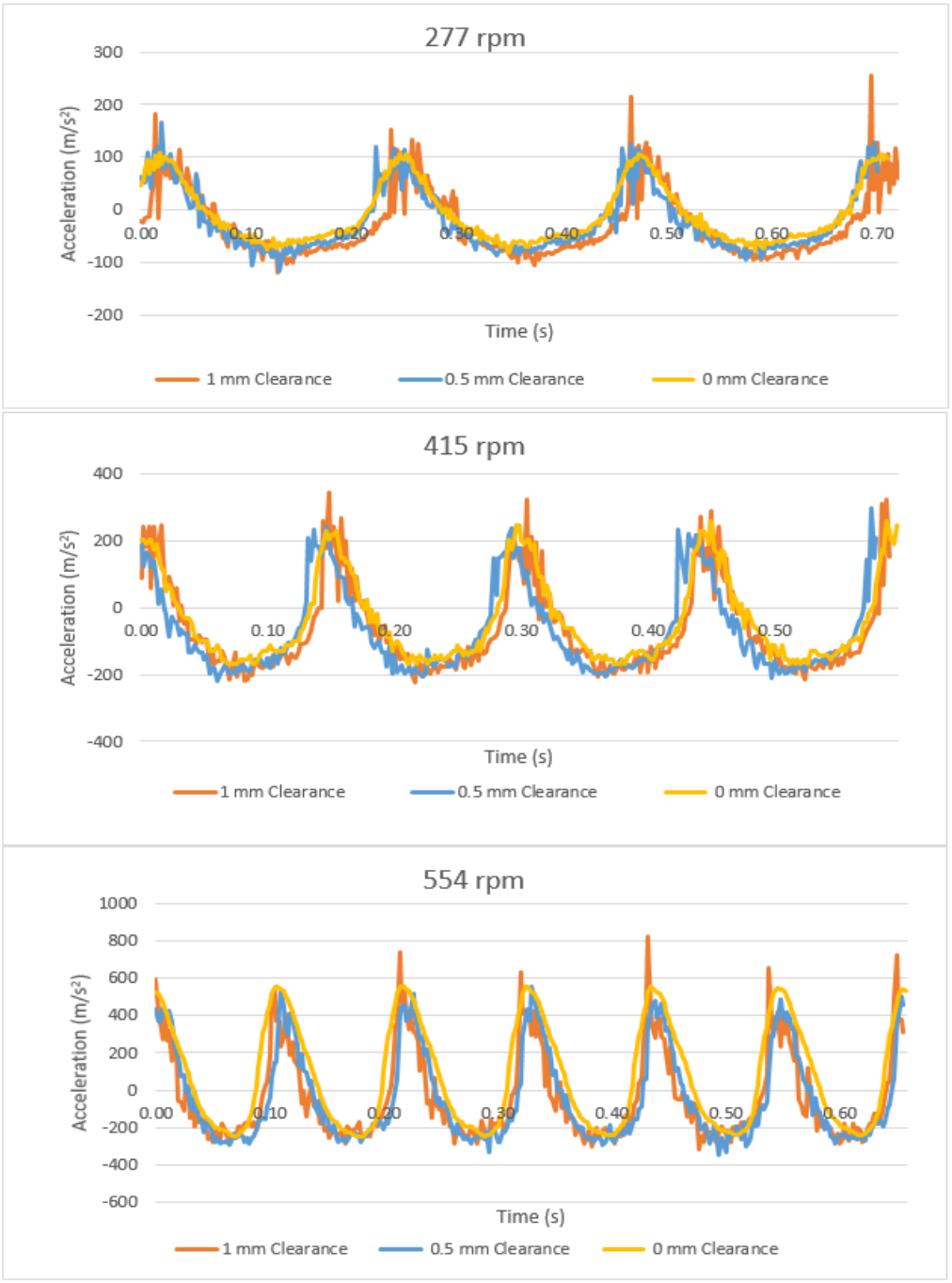

Figure 57: Experimental acceleration results for steel-1.5 mm at three speeds (three clearance sizes)

5.1.5 The difference between rigid and flexible mechanisms. To highlight the effect of the flexibility on the mechanism with joint clearance; the follower acceleration results using the rigid coupler are plotted with each one of flexible coupler links at the three crank speeds. In this section, only the exaggerated size of clearance 1 mm is considered in order to emphasize the difference between the flexible and the rigid mechanisms, and to outline the most effective case of mentioned flexible couplers.

Rigid case with aluminuim-4 mm:

Figure 58 shows that the aluminum with 4 mm thickness provided better results than the steel with 5 mm thickness as it has one peak per cycle at the speed of 277 rpm and 415 rpm compared to two remarkable peaks per cycles for the rigid case. However, at the highest speed, 554 rpm the results show the occurrence of small two peaks per cycle, which is due to the thickness 4 mm that is almost rigid.

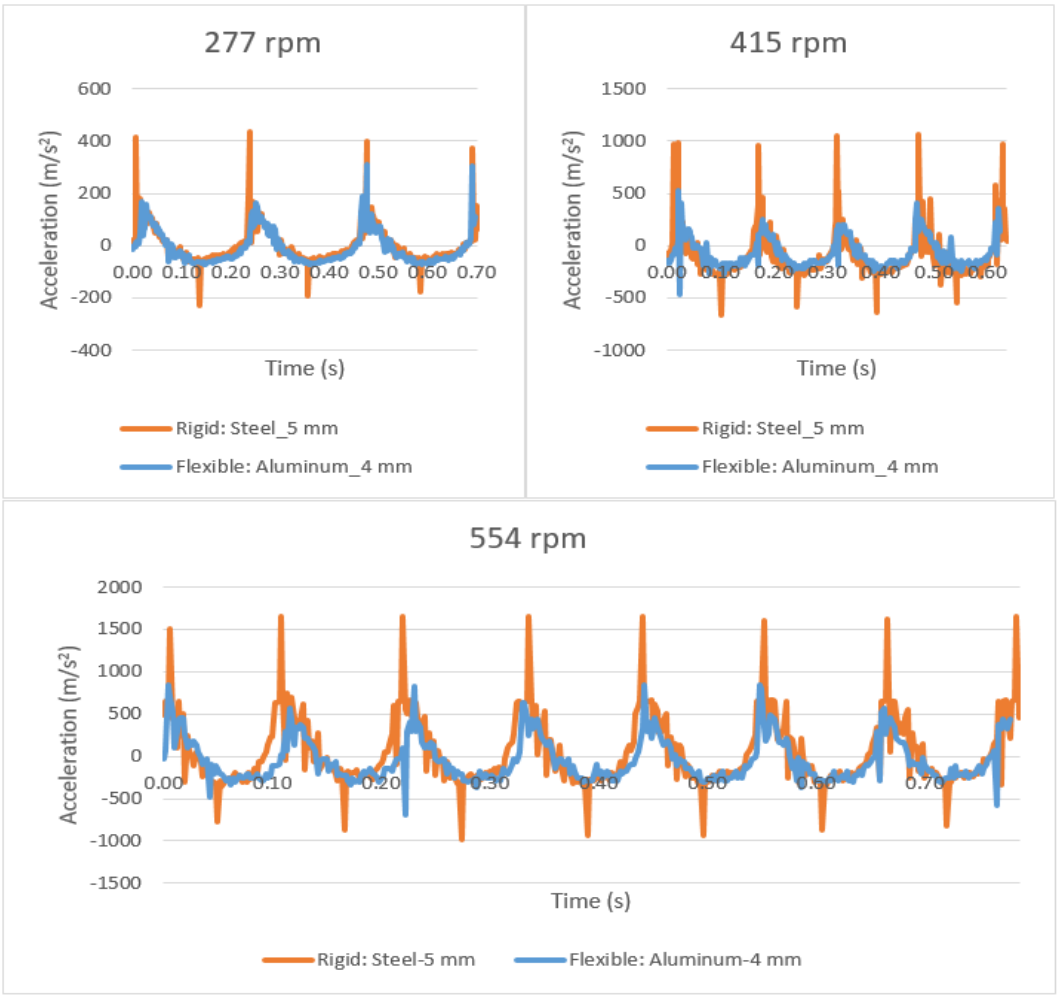

Figure 58: Experimental results of 1mm clearance for the steel-5 mm and aluminuim-4 mm (three speeds)

It can be observed that for the rigid case in Figure 58, peaks of 400 m/s^2 are measured at 277 rpm, which increased to almost 1000 m/s^2 at 415 rpm and increased further to slightly higher than 1500 at 554 rpm. The peaks indicate the occurrence of impacts.

Rigid case with aluminuim-3 mm:

It can be noticed from Figure 59 that using aluminum with 3 mm thickness provides better results than aluminum-4 mm thickness as it has smaller number and values of peaks. Compared to the rigid case, using aluminum with 3 mm thickness results in almost eliminating the impacts and providing smoother results.

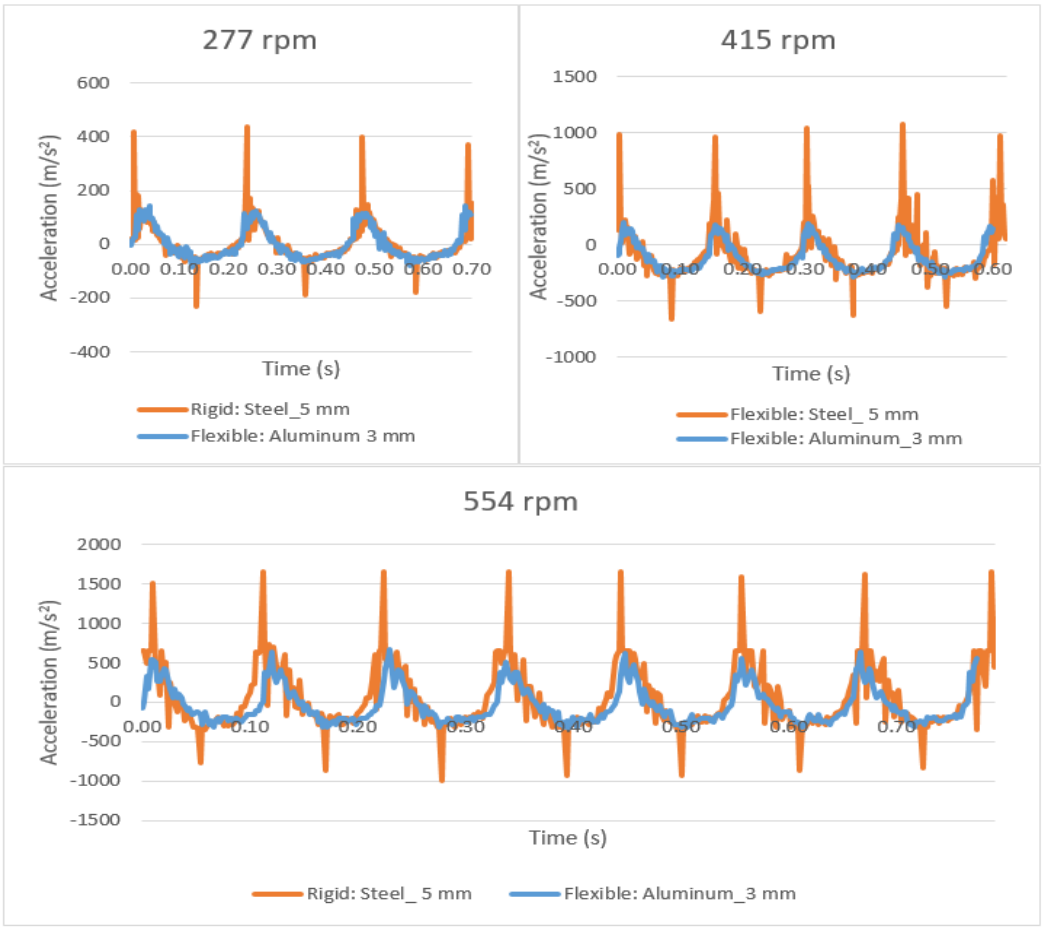

Figure 59: Experimental results of 1mm clearance for the steel-5 mm and aluminuim-3 mm (three speeds)

Rigid case with Steel-2 mm:

For the steel with 2 mm thickness, the results show almost similar results like the previous case (aluminum with 3 mm thickness). The obtained results show that there is one small peak per cycle for the three speeds compared to the remarkable peaks of

the rigid case (Figure 60). The acceleration values for steel with 2 mm thickness increased from 200 m/s^2 at 277 rpm to 400 m/s^2 at 415 rpm up to 800 m/s^2 at 554 rpm.

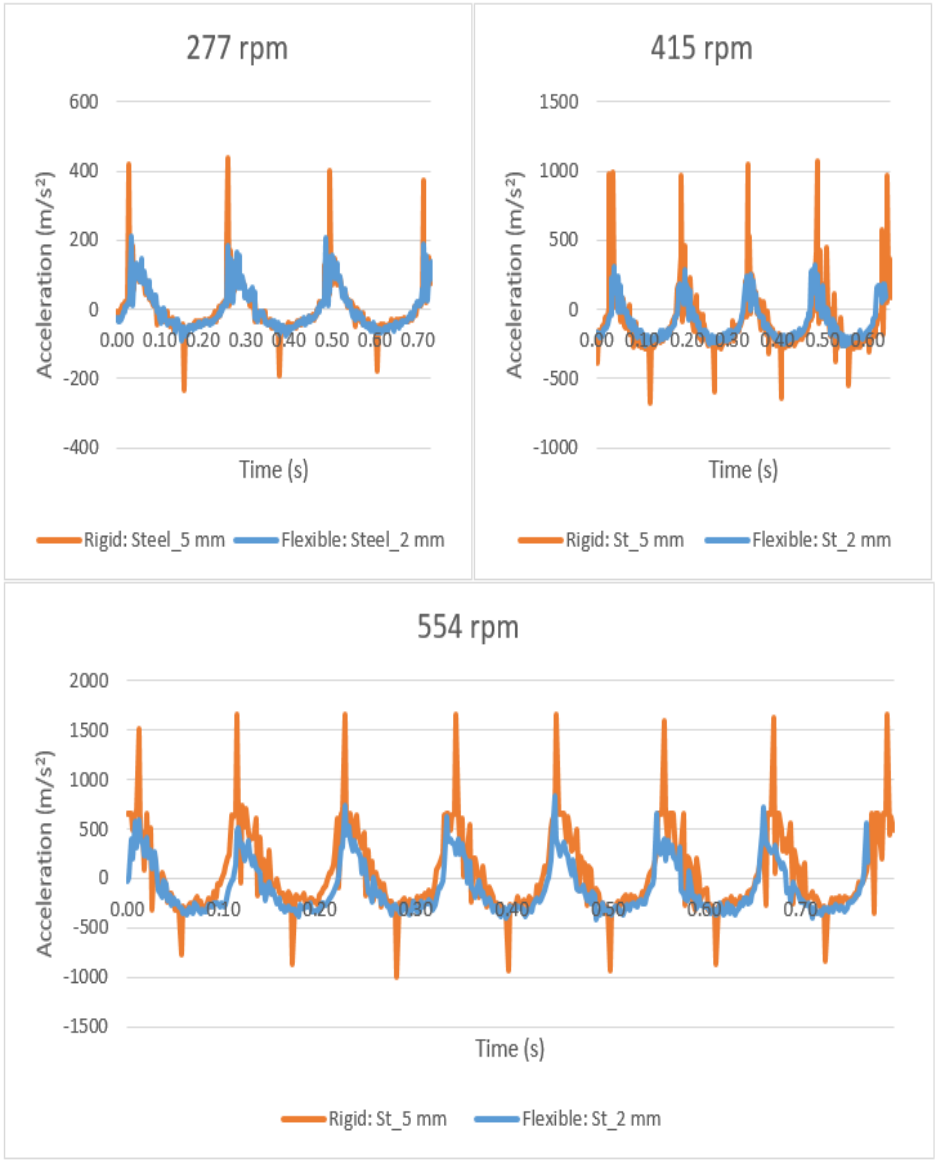

Figure 60: Experimental results of 1mm clearance for the steel-5 mm and steel-2 mm (three speeds)

Rigid case with Steel-1.5 mm:

For steel with 1.5 mm thickness, the obtained results in Figure 61 show that, there are two peaks for each cycle with smaller values of the acceleration compared to the rigid case. The reason of having more peaks than the other flexible couplers is that the thickness of the coupler is very small and the deformation in the link is nearly plastic as explained in Chapter 4.

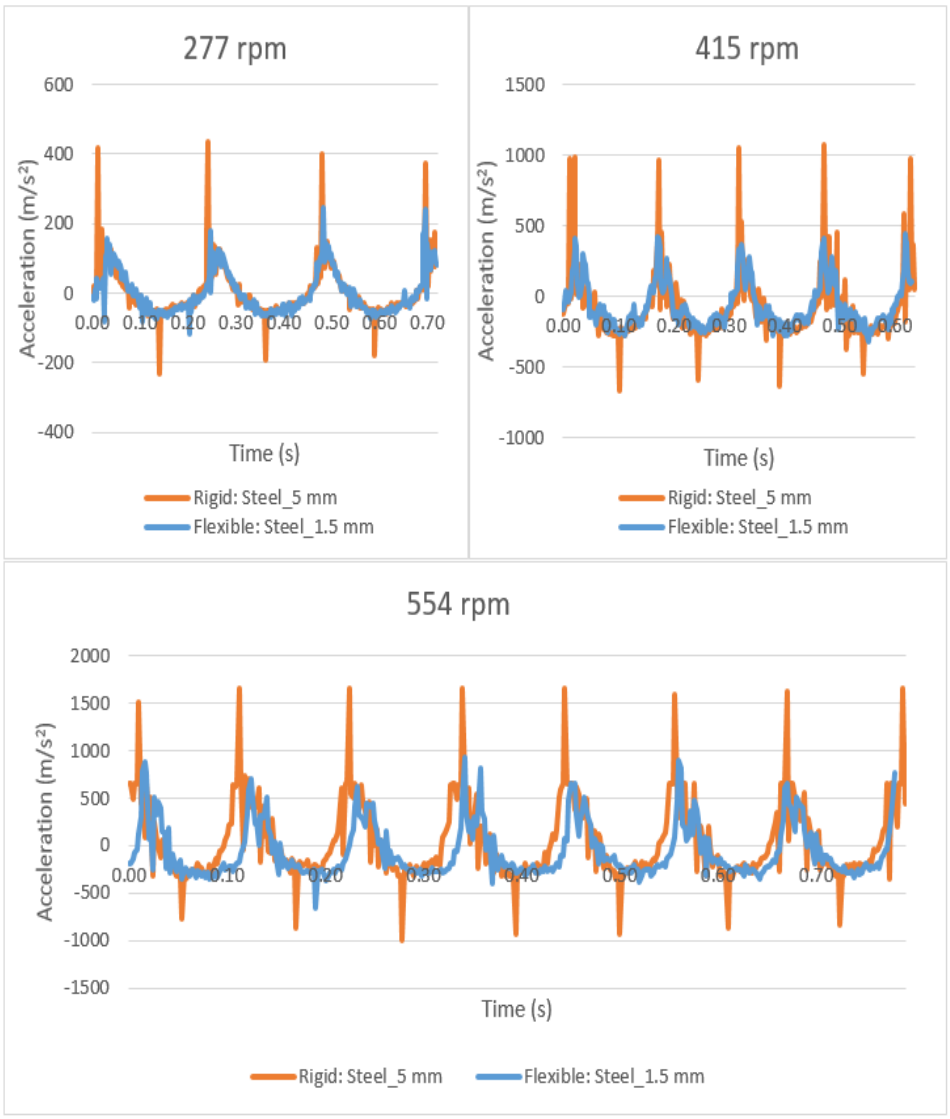

Figure 61: Experimental results of 1mm clearance for the steel-5 mm and steel-1.5 mm (three speeds)

5.2 Simulation Setup

In order to validate the experimental results, the model is built using ADAMS software with the same characteristics as the one used in Chapter 4. The clearance then is added in the joint between the coupler and the follower (Figure 62).

5.2.1 Clearance modeling in ADAMS. To model the clearance in the joint using ADAMS few steps should be considered as shown in Figure 63 :

1. First the revolute joint -that connects the coupler and the follower- is disabled in order to add the clearance manually.
2. A cylinder is added and connected to the coupler with revolute joint with a diameter of 7 mm.

3. Another cylinder is added to the follower with a hole in the middle of 8 mm, where the coupler's cylinder goes inside.
4. The diameter of the inside cylinder is then modified according to the clearance size.

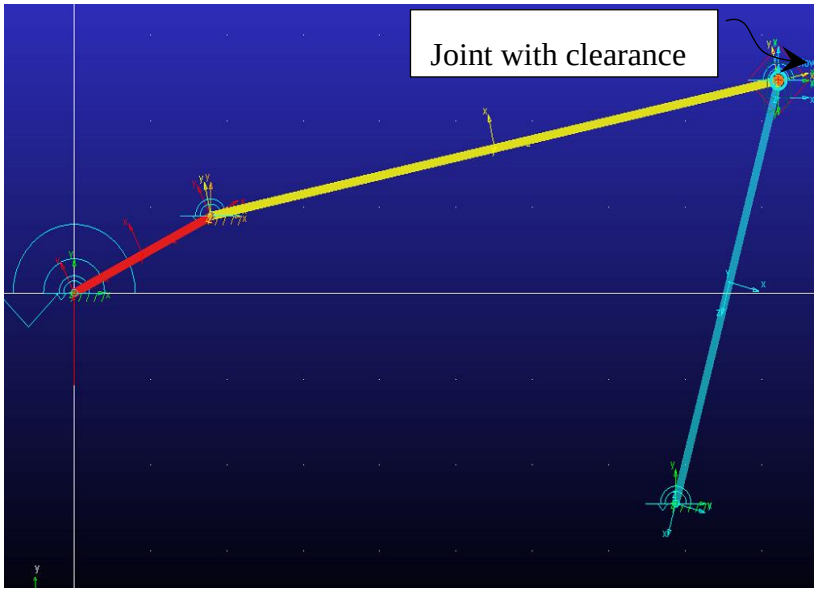

Figure 62: Four-bar mechanism (built using ADAMS software) with join clearance.

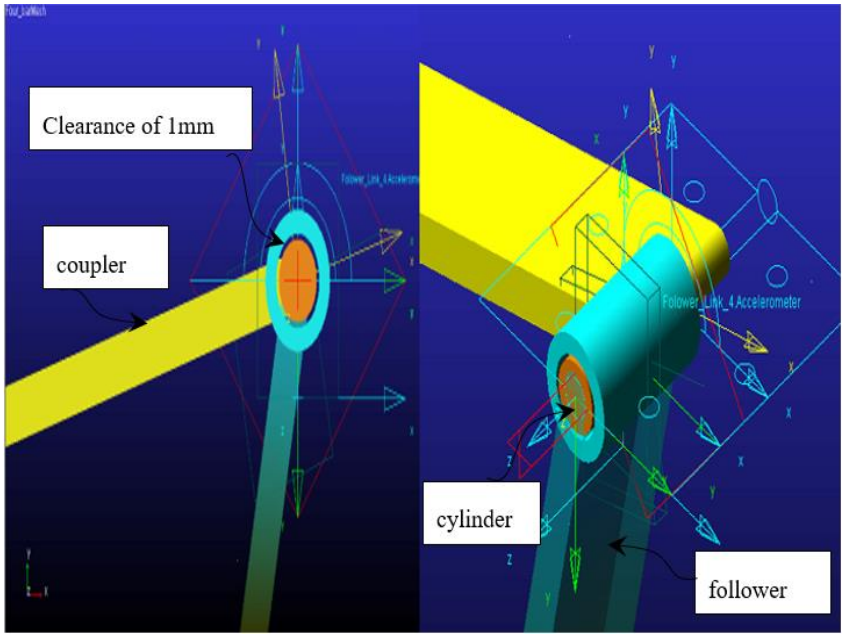

Figure 63: Modeling the clearance under ADAMS

It is interesting to indicate that there is an alternative method of modeling the clearance using ADAMS by adding two circles; one for the coupler and the other for the follower -at the joint location- with different diameters where the difference is equal to the required clearance size.

5.2.2 Contact modeling. As a result of disabling the revolute joint, the contact between the coupler and the follower is lost. Therefore, the contact should be modeled which is done using impact function method. The contact force is calculated using ADAMS/solver from the IMPACT function in the ADAMS function library. This contact force model is proved to compensate for the energy dissipation along the impact motion period [31].

In order to model the contact under ADAMS some of the parameters should be calculated first. The following equations are derived from [13]:

$$F_N = \begin{cases} K\delta^n + STEP(\delta,0,0,d_{\max},C_{\max})\dot{\delta}, \rightarrow \delta > 0 \\ 0, \rightarrow \delta \le 0 \end{cases} \tag{20}$$

$$K = \frac{4}{3\pi(h_i + h_j)} * \left(\frac{R_i R_j}{R_i + R_j} \right)^{1/2} \tag{21}$$

$$STEP(\delta,0,0,d_{\max},C_{\max}) = \begin{cases} 0 \rightarrow \delta \le 0 \\ C_{\max}\left(\frac{\delta}{d_{\max}}\right)^2 \left(3 - 2\frac{\delta}{d_{\max}}\right) \rightarrow 0 < \delta < d_{\max} \\ C_{\max} \rightarrow \delta \ge d_{\max} \end{cases} \tag{22}$$

where:

F_N is The normal force of the contact (N).

K is the stiffness coefficient (N/m).

δ is the normal penetration depth at the contact point (mm).

$C_{\max}$ is maximum damping coefficient.

d_{max} is the positive real value specifying the boundary penetration (mm).

$R_{i,j}$ are the radius of the journal and sleeve (mm).

$h_{i,j}$ are constants that depend on the modulus of the elasticity and Poisson's ratio of the material.

The contact type should be defined regarding the method used in modeling the clearance. It should be defined as solid to solid when the contact elements are rigid and solid to flexible if one of the elements is rigid and the other is flexible. However, using

the circle method, the contact type should be defined as curve to curve. Figure 64 shows the parameters defined in ADAMS for modeling the contact and the contact type set as solid to solid. The other parameters are found in the literature [32].

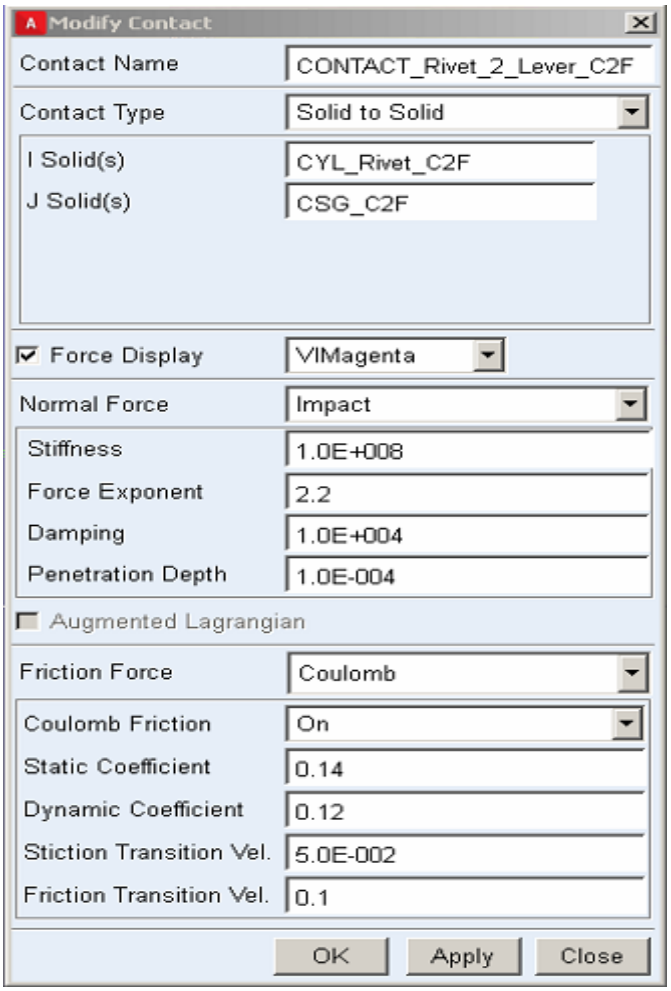

Figure 64: The contact parameters defined in ADAMS.

5.3 Simulation Results

In this section, some of the simulation results are presented for the flexible and rigid mechanisms with the experimental results using the three defined clearance sizes for the case of the highest speed 554 rpm as it overstresses the effect of clearance.

5.3.1 Rigid case (steel-5 mm). Figure 65 shows the experimental and ADAMS acceleration results for the rigid case (steel-5mm). It can be noticed that the experimental and ADAMS results show the same trends, where two peaks appear each cycle. However, the experimental results show more fluctuation than the simulation results. This is due to the accelerometer being sensitive to noise.

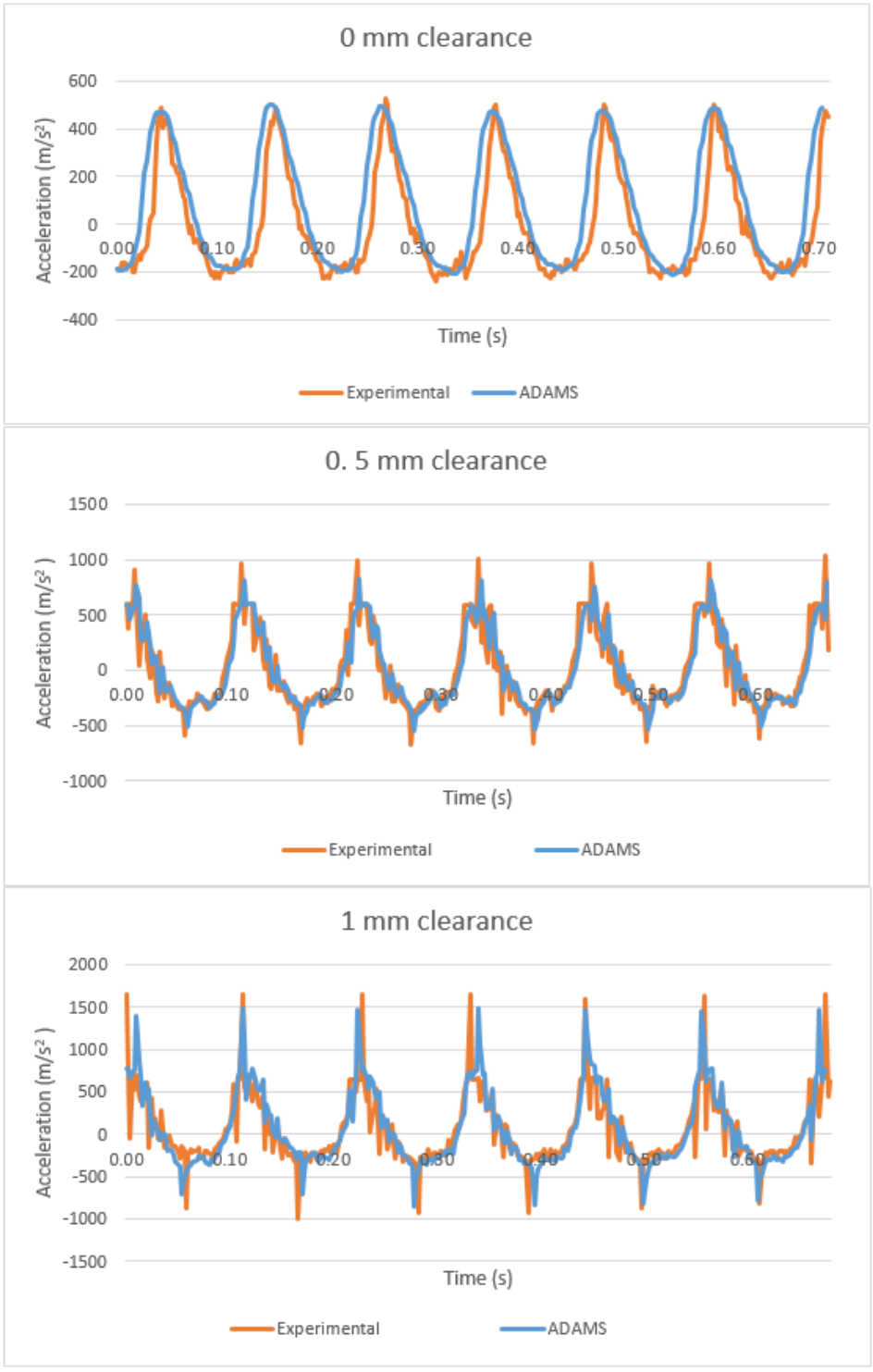

Figure 65: Experimental and Simulation acceleration results for steel 5 mm at 554 rpm (three clearance sizes)

5.3.2 Flexible case. In this section the experimental acceleration results using the different defined flexible coupler links are obtained with ADAMS results at the highest speed 554 rpm -using the three clearance sizes- as shown from Figure 66 to

Figure 69. It can be noticed that the results of ADAMS and the experimental results are quite similar.

Although using aluminum with 4 mm thickness highly enhances the acceleration results compared to the rigid case, the obtained results in Figure 65 indicates the occurrence of impact as shown in Figure 66.

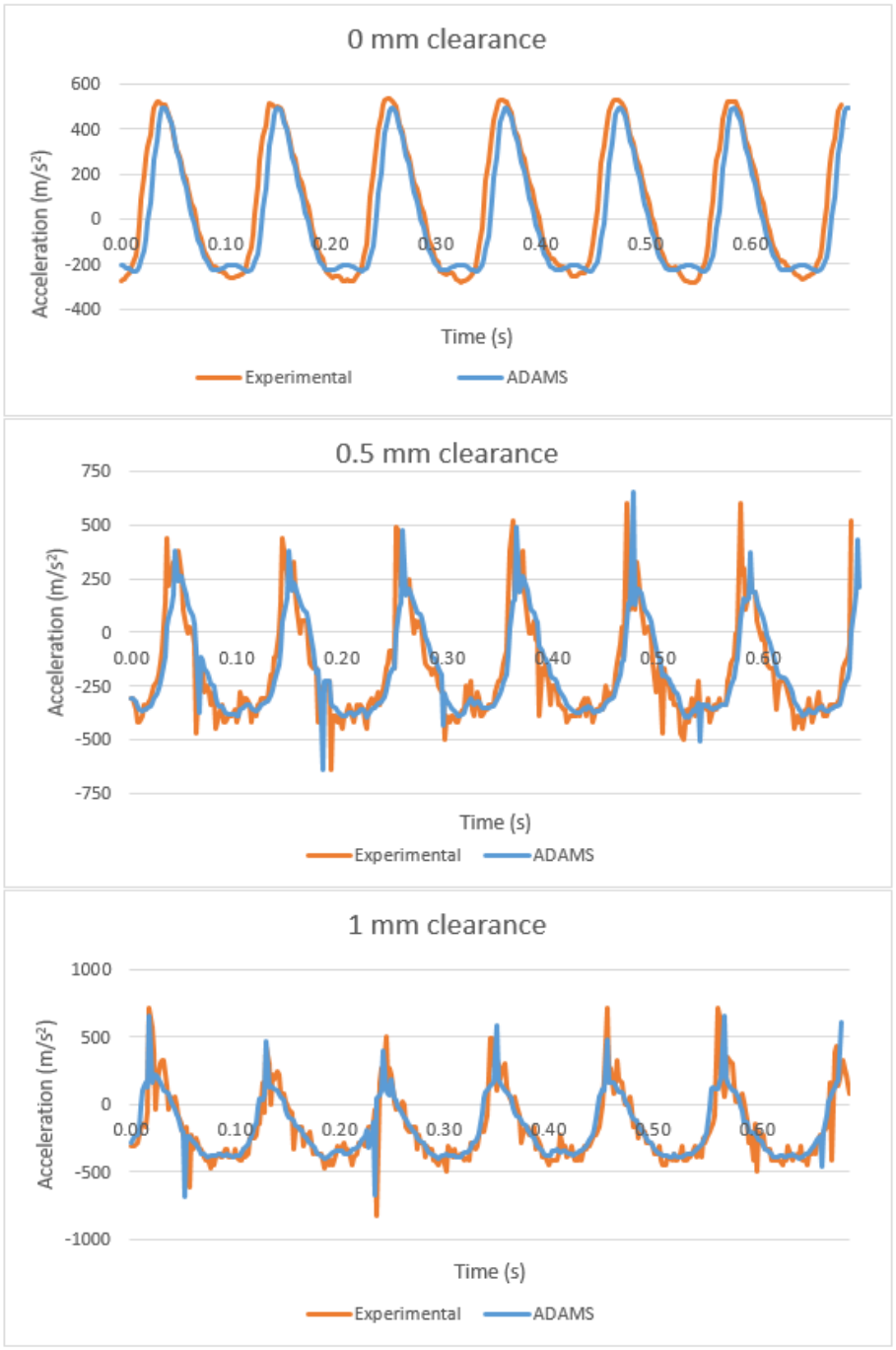

Figure 66: Experimental and Simulation acceleration results for aluminum 4 mm at 554 rpm (three clearance sizes)

On the other hand, ADAMS and the experimental results shown in Figure 67 proved that using aluminum-3 mm provides results similar to the mechanism with ideal joints, where only small peaks appear for the case of 1 mm at the highest crank speed 554 rpm.

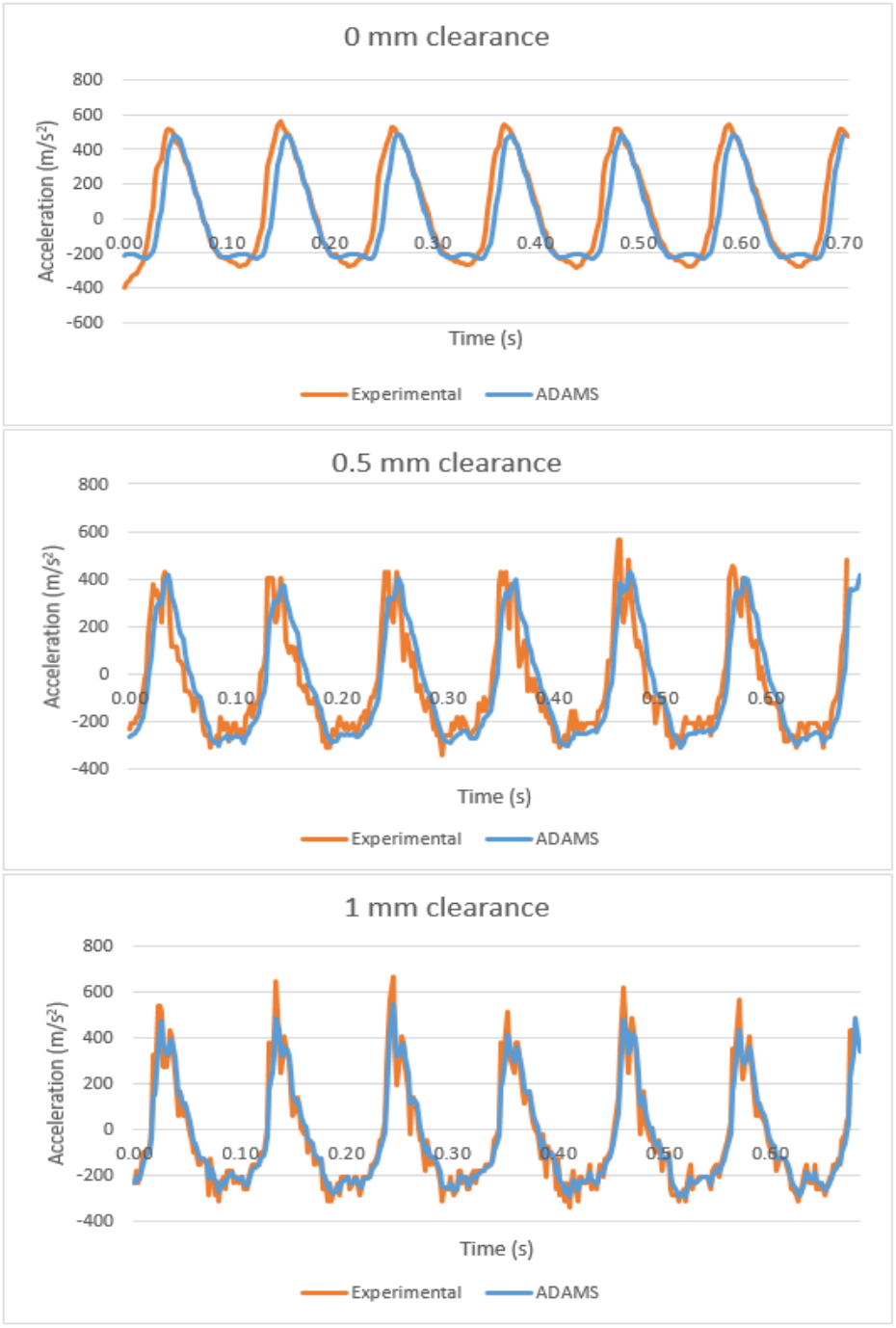

Figure 67: Experimental and Simulation acceleration results for aluminum 3 mm at 554 rpm (three clearance sizes)

Using Steel with 2 mm also yields good results with only one small peak per cycle as shown in Figure 68.

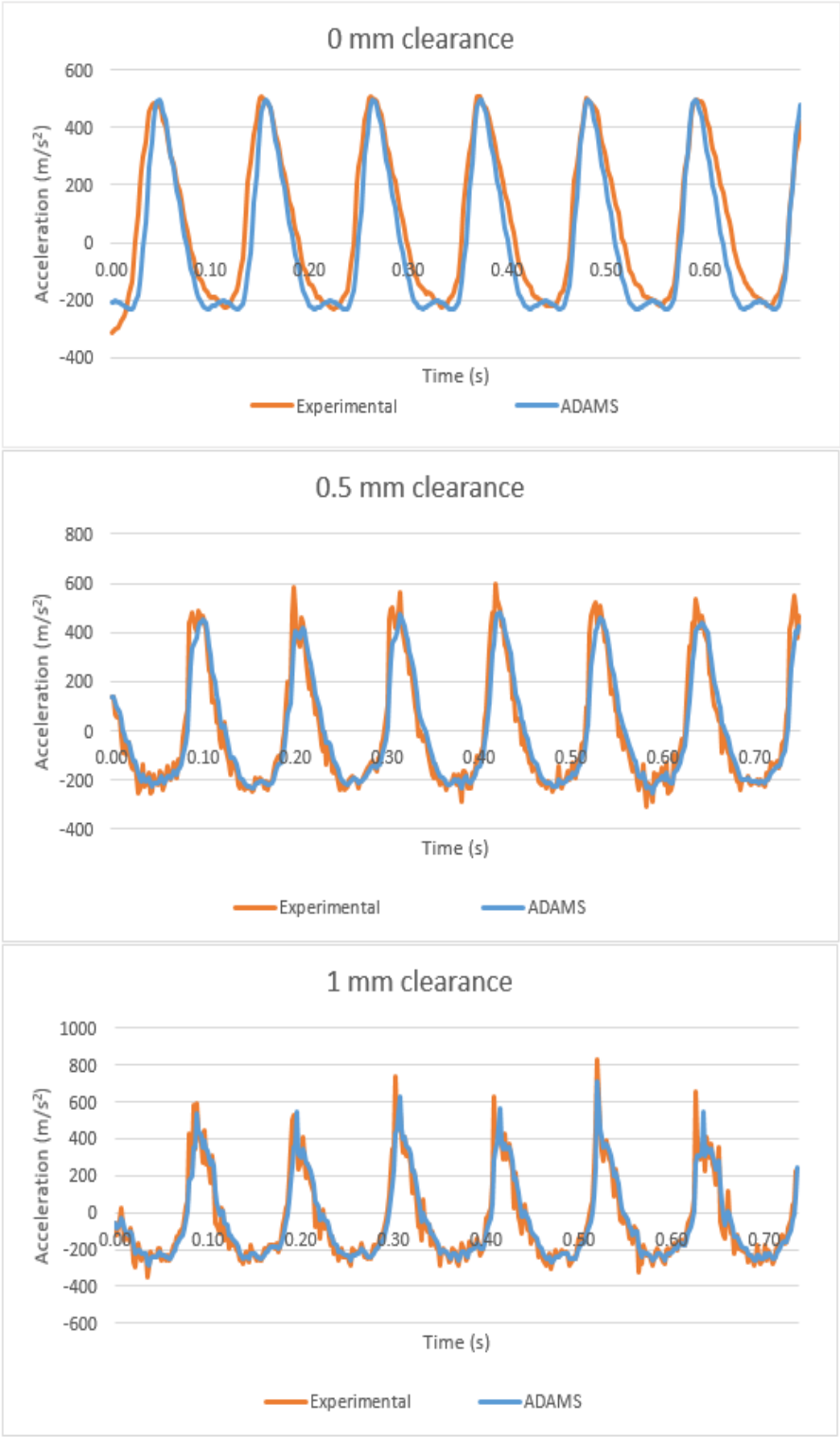

Figure 68: Experimental and Simulation acceleration results for steel 2 mm at 554 rpm (three clearance sizes)

The acceleration results of steel 1.5 mm case show the occurrence of small peaks which is clarified by the small thickness of the link, as shown in Figure 69.

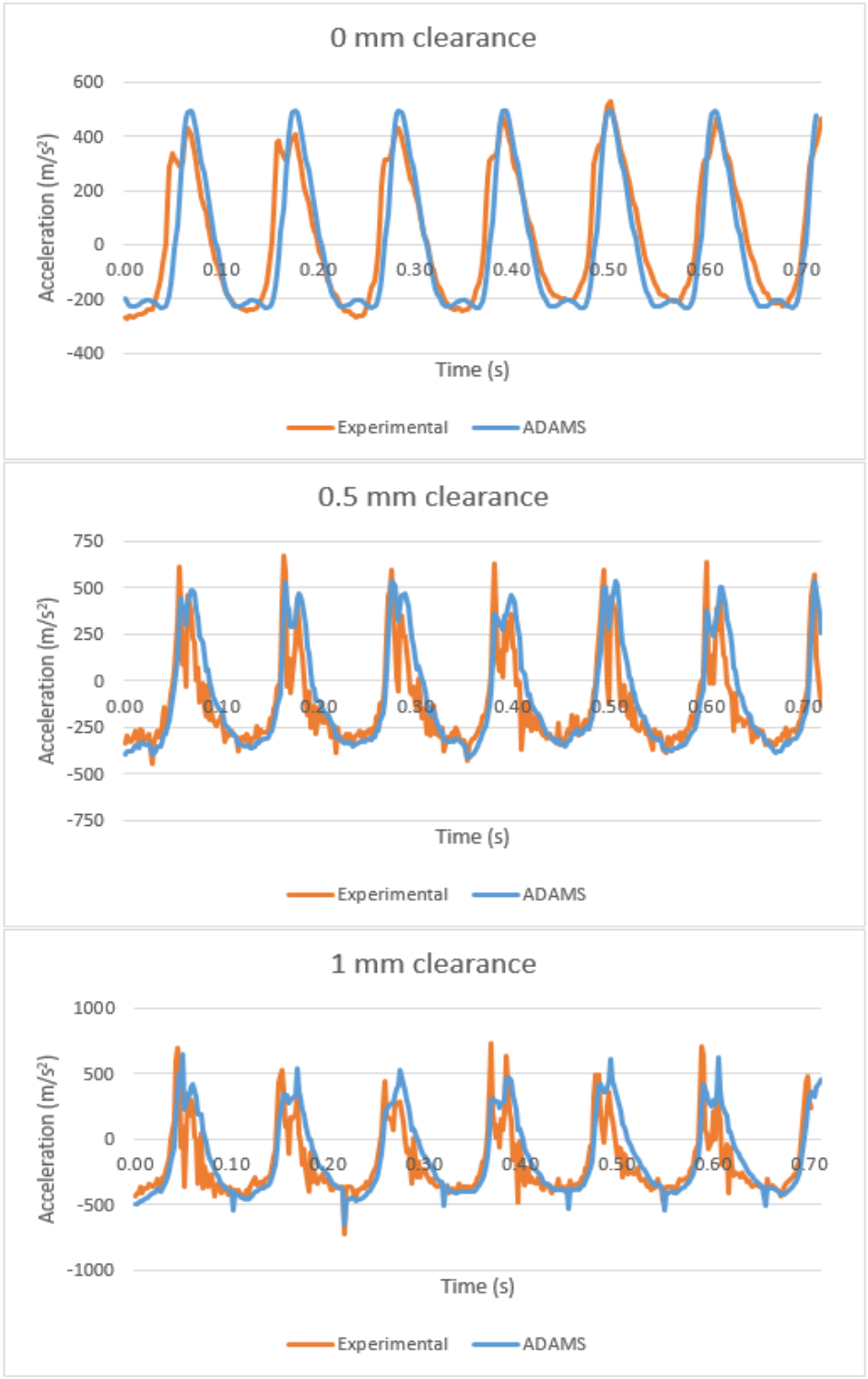

Figure 69: Experimental and Simulation acceleration results for steel 1.5 mm at 554 rpm (three clearance sizes)

5.3.3 Contact force results. Since the simulation results show almost the same trend like the experimental ones; the horizontal and vertical contact forces are measured using ADAMS software. The obtained results shown in this section are for the rigid case (steel with 5 mm thickness) and flexible case; aluminum coupler with 3 mm thickness and steel with 2 mm thickness at 554 rpm using the exaggerated clearance size 1 mm.

Rigid case (steel-5 mm):

Figure 70 shows the horizontal and vertical components of the contact force using the steel with 5 mm thickness coupler. It can be observed that two impacts are detected per cycles. The impacts have fluctuations which are due to bouncing and friction within the joint. It is worth mentioning that the force of impacts has further effects on the y-direction than the x-direction, as it reached 400 N for the prior compared to 250 N for the later.

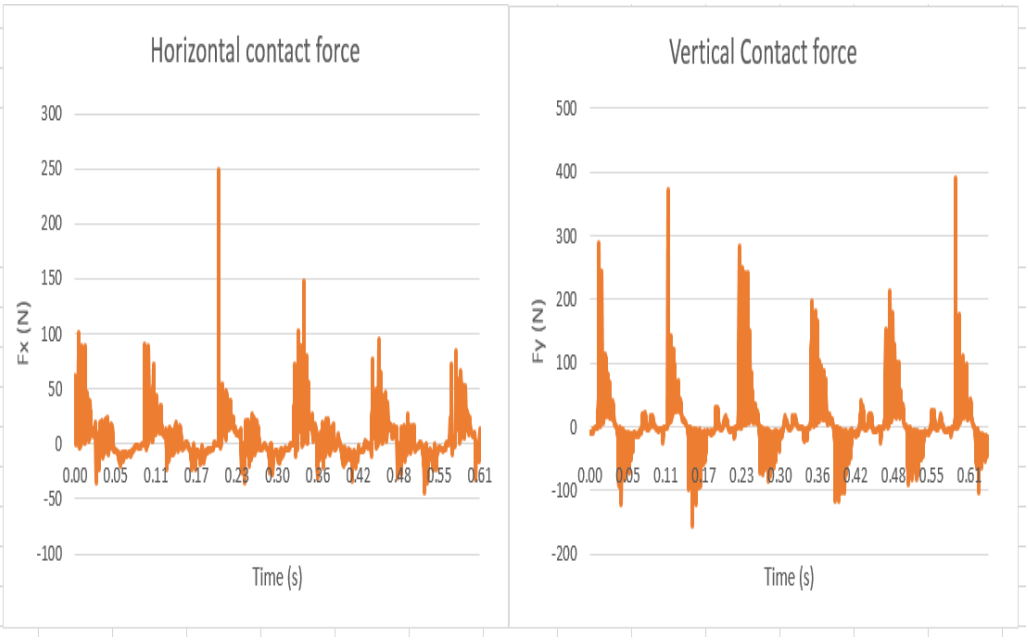

Figure 70: Horizontal and vertical components of the contact force for steel 5 mm (Simulation results)

Flexible case (aluminum-3 mm and steel-2mm):

For the aluminum with 3 mm thickness and steel with 2 mm thickness couplers, the contact force results show better behavior, where the number of impacts decreased and they maintained for short time interval compared to the rigid case as shown in Figure 71 and Figure 72. One can notice that the results of both flexible mechanisms show almost similar trends and values of contact forces.

Figure 71: Horizontal and vertical components of the contact force for aluminum 3 mm (Simulation results)

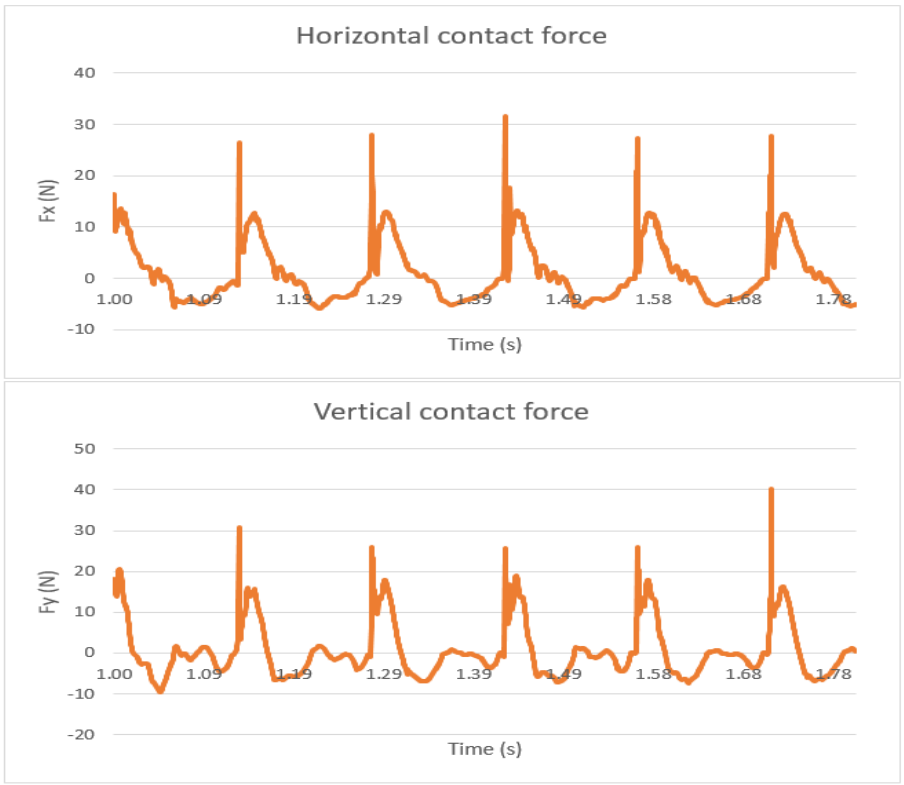

Figure 72: Horizontal and vertical components of the contact force for steel 2 mm (Simulation results)

In conclusion, the effect of the crank speed, the clearance size and the link flexibility on the mechanism behavior is investigated. The obtained results show that, as the crank speed and the clearance size increase, the acceleration values and the number of impacts increase significantly. Also, using flexible couplers enhances the mechanism dynamic responses (accelerations and contact forces), significantly. The experimental results are confirmed by ADAMS simulation results and they show a good agreement.

Chapter 6: Conclusion and Future Work

The dynamic behavior of a four-bar mechanism with clearance was investigated through simulations and experiments using rigid and flexible mechanisms. The four-bar mechanism consists of 4 revolute joints and a crank (driven link), a coupler and a follower. The presence of clearance in the joint between the coupler and the follower induces three types of motions; impacts, free flight (no contact) and permanent contact (continuous contact between the journal and sleeve). This results in vibration, noise and decreasing of the mechanism efficiency. The simulation for the case of rigid four-bar mechanism was carried out using MATLAB software. To be able to predict the occurrence of the impact in simulation results, a condition, based on monitoring the moment of the reaction force in the joint with clearance, was derived. Two impacts (peaks) per crank's revolution were predicted and validated experimentally. In order to eliminate these impacts two methods were proposed.

- The first method was based on attaching a spring between the coupler and the follower. Using this method, it was shown that the impact could be easily eliminated using adequate spring parameters. However, this modification resulted in a higher maximum input torque and an increase of its fluctuation. An optimization of the spring parameters, using MATLAB, was then performed to keep the beneficial effects of the spring (eliminating impacts) and to minimize its bad effects on the torque.
- The second proposed solution aimed at studying the dynamic behavior of the four-bar mechanism with clearance and flexible links. The dynamic analysis of the flexible mechanism was investigated using two different materials of the coupler link (aluminum and steel) with two different thickness values for each material (3 and 4 mm for aluminum and 1.5 and 2 mm for the steel). The rigid mechanism was considered in this case with a coupler link made of steel with 5 mm thickness.
- The deformation of the flexible coupler links using ideal joints was investigated through experiments and validated with simulation tests using ADAMS software. The strain values were measured in the mid-point of the coupler at three different speeds (277 rpm, 415 rpm and 554 rpm). The obtained results

illustrate that the strain values are significantly affected by the speed and the thickness of the links.

- The accelerations of a point on the follower were measured through experimental tests for the four-bar mechanism using rigid and flexible coupler links. These measurements were performed for the case of an ideal joint (no clearance) and a realistic joint with a clearance of 0.5 mm and 1 mm at three different speeds.
- The experimental results were validated through simulation tests, which were done using ADAMS software. They confirm that the flexibility of the coupler plays a role of a suspension for the mechanism. The experimental and simulation results showed a good agreement.

The dynamic behavior of mechanisms with multi-joints with clearance could be considered as a future work. In order to capture the dynamic behavior of a multibody mechanical system precisely, all the joints in the system should be modeled with clearance in future works. It is recommended to use a flexible mechanism and lubricated joints in order to eliminate totally the effect of the clearance.

References

[1] F. Meng, S. Wu, F. Zhang, and L. Liang, "Numerical Modeling and Experimental Verification for High-Speed and Heavy-Load Planar Mechanism with Multiple Clearances," *Mathemetical Probl. Eng.*, vol. 2015, pp. 1–11, 2015.

[2] J.-S. Chen and K.-L. Chen, "The Role of Lagrangian Strain in the Dynamic Response of a Flexible Connecting Rod," *J. Mech. Des.*, vol. 123, no. 4, pp. 542–548, 2001.

[3] W. Xu-peng and L. Geng, "Science Direct Study on Impact Dynamics of Development for Solar Panel with Cylindrical Clearance Joint," *Procedia Eng.*, vol. 2014, pp. 1–13, 2014.

[4] X. Li, X. Ding, and G. S. Chirikjian, "Analysis of Angular-Error Uncertainty in Planar Multiple-Loop Structures with Joint Clearances," *Mech. Mach. Theory*, vol. 91, pp. 69–85, 2015.

[5] A. Armillotta, "Force Analysis as A Support to Computer-aided Tolerancing of Planar Linkages," *Mech. Mach. Theory*, vol. 93, pp. 11–25, 2015.

[6] S. M. Megahed and A. F. Haroun, "Analysis of the Dynamic Behavioral Performance of Mechanical Systems With Multi–Clearance Joints," *J. Comput. Nonlinear Dyn.*, vol. 7, no. 1, pp. 1–11, 2012.

[7] Z. Bai, B. Yang, and Y. Sun, "Investigation on Dynamics of Mechanical System with Clearance Joint," *Open Mech. Eng. J.*, pp. 224–229, 2014.

[8] M. Dupac and D. G. Beale, "Dynamic Analysis of a Flexible Linkage Mechanism with Cracks and Clearance," *Mech. Mach. Theory*, vol. 45, no. 12, pp. 1909–1923, 2010.

[9] S. M. Varedi, H. M. Daniali, M. Dardel, and A. Fathi, "Optimal Dynamic Design of a Planar Slider-Crank Mechanism with a Joint Clearance," *Mech. Mach. Theory*, vol. 86, pp. 191–200, 2015.

[10] P. Flores and H. M. Lankarani, "Dynamic Response of Multibody Systems with Multiple Clearance Joints," *J. Comput. Nonlinear Dyn.*, vol. 7, no. 3, pp. 3–13, 2012.

[11] S. Erkaya and I. Uzmay, "Determining Link Parameters Using Genetic Algorithm in Mechanisms with Joint Clearance," *Mech. Mach. Theory*, vol. 44, no. 1, pp. 222–234, 2009.

[12] P. Taylor, Y. Chen, and J. Lu, "Minimise Joint Clearance in Rapid Fabrication of Non- Assembly Mechanisms," *Int. J. Comput. Integr. Manuf.*, vol. 24, no.

January 2015, pp. 37–41, 2011.

[13] I. Khemili and L. Romdhane, “Dynamic Analysis of a Flexible Slider-Crank Mechanism with Clearance,” *Eur. J. Mech. A/Solids*, vol. 27, no. 5, pp. 882–898, 2008.

[14] J. Chunmei, Q. Yang, F. Ling, and Z. Ling, “The Non-Linear Dynamic Behavior of an Elastic Linkage Mechanism With Clearances,” *J. Sound Vib.*, vol. 249, no. 2, pp. 213–226, 2002.

[15] E. Zheng and X. Zhou, “Modeling and Simulation of Flexible Slider-Crank Mechanism with Clearance for a Closed High Speed Press System,” *Mech. Mach. Theory*, vol. 74, pp. 10–30, 2014.

[16] S. Erkaya and I. Uzmay, “Effects of Balancing and Link Flexibility on Dynamics of a Planar Mechanism having Joint Clearance,” *Sci. Iran.*, vol. 19, no. 3, pp. 483–490, 2012.

[17] S. Erkaya, “Prediction of Vibration Characteristics of a Planar Mechanism Having Imperfect Joints Using Neural Network,” *J. Mech. Sci. Technol.*, vol. 26, no. 5, pp. 1419–1430, 2012.

[18] V. L. Reis, G. B. Daniel, and K. L. Cavalca, “Dynamic Analysis of a Lubricated Planar Slider-Crank Mechanism Considering Friction and Hertz Contact Effects,” *Mech. Mach. Theory*, vol. 74, pp. 257–273, 2014.

[19] Q. Tian, Y. Zhang, L. Chen, and P. Flores, “Dynamics of Spatial Flexible Multibody Systems with Clearance and Lubricated Spherical Joints,” *Comput. Struct.*, vol. 87, no. 13–14, pp. 913–929, 2009.

[20] Z. Hai-yang, X. Min-qiang, W. Jin-dong, and L. Yong-bo, “A parameters Optimization Method for Planar joint Clearance Model and its Application for Dynamics Simulation of Reciprocating Compressor,” *J. Sound Vib.*, vol. 344, pp. 416–433, 2015.

[21] M. S. Feki, F. Chaari, M. S. Abbes, F. Viadero, a. Fdez. Del Rincon, and M. Haddar, “New Trends in Mechanism and Machine Science,” *Mech. Mach. Sci.*, vol. 7, pp. 311–318, 2013.

[22] D. F. L. Senevirate, S. Earles, “Analysis of a Four-Bar Mechanism with a Radially Compliant Clearance Joint,” *Institutution Mech. Eng.*, vol. 210, pp. 215–223, 1996.

[23] T. Li, J. Guo, and Y. Cao, “Dynamic Characteristics Analysis of Deployable Space Structures Considering Joint Clearance,” *Acta Astronaut.*, vol. 68, no. 7–8, pp. 974–983, 2011.

[24] Z. Feng Bai, Y. Zhao, and J. Chen, “Dynamics Analysis of Dual-Axis Positioning Mechanism of Satellite Antenna with Joint Clearance,” *Multidiscip.*

Model. Mater. Struct., vol. 10, no. 1, pp. 59–74, 2014.

[25] A. Azimi Olyaei and M. R. Ghazavi, "Stabilizing Slider-Crank Mechanism with Clearance Joints," *Mech. Mach. Theory*, vol. 53, pp. 17–29, 2012.

[26] S. Rahmanian and M. R. Ghazavi, "Bifurcation in Planar Slider–Crank Mechanism with Revolute Clearance Joint," *Mech. Mach. Theory*, vol. 91, pp. 86–101, 2015.

[27] X. Jia, D. Jin, L. Ji, and J. Zhang, "Investigation on the Dynamic Performance of the Tripod-Ball Sliding Joint With Clearance in a Crank–Slider Mechanism. Part 1. Theoretical and Experimental Results," *J. Sound Vib.*, vol. 252, no. 5, pp. 919–933, 2002.

[28] R. L. Norton and J. M. McCarthy, *Design of Machinery*, The USA: McGraw-Hill, 2003, pp. 144-165.

[29] S. Yaqubi, M. Dardel, H. M. Daniali, and M. Hassan, "Nonlinear Dynamics and Control of Crank-Slider Mechanism with Multiple Clearance Joints," *Theor. Appl. Vib. Acoust.*, vol. 1, pp. 21–31, 2015.

[30] D. M. Ştefănescu, "Strain Gauges and Wheatstone Bridges - Basic Instrumentation and New Applications for Electrical Measurement of Non-Electrical Quantities," *Int. Multi-Conference Syst. Signals Devices, Romania*, 2011.

[31] M. A. Ben Abdallah, I. Khemili, and N. Aifaoui, "Numerical Investigation of a Flexible Slider–Crank Mechanism with Multijoints with Clearance," *Multibody Syst. Dyn.*, vol. 37, no. 3, pp. 1–29, 2016.

[32] X. Yao, X. Guo, Y. Feng, C. Yu, and C. Ma, "Dynamic Analysis for Planar Beam with Clearance Joint," *J. Sound Vib.*, vol. 339, pp. 324–341, 2015.

Vita

Mona Albashir is Sudanese who was born in 1988 in Saudi Arabia. She graduated from university of Khartoum in 2009 with a Bachelor of Science in Mechanical engineering and she was awarded the prize of the best senior design project with her other three peers.

After graduation Ms. Mona worked at Asawer Oil and Gas Company in Sudan for almost four years. In 2014 she joined the American University of Sharjah as a graduate teaching assistant to start her Master program in Mechanical Engineering.